Universitat
Autònoma
de Barcelona

REAL-TIME SIGN CLASSIFICATION FOR AIBO ROBOTS

Memòria del Projecte Fi de Carrera
d'Enginyeria en Informàtica
realitzat per
José Luis Ledesma Piqueras
Director: Sergio Escalera
Tutora: Petia Radeva
Bellaterra 12 de Juny de 2006

Last years robotics intelligence has shown significant improvement due to the high quality of the actual technology. Based on last advances of Computer Vision, intelligent systems have been designed to allow the robotics devices to simulate autonomous behaviors. In this paper, we design a real-time model matching and classification system in order to allow an Aibo robot to interact with its environment. The experiments show good performance on synthetic objects recognition in cluttered scenes, and simulate autonomous behaviors in non-controlled environments. Besides, we extend our system to run in real traffic sign recognition system. In different real experiments, our application shows a good performance being robust either in case of lack of visibility, partial occlusions, illumination changes and slightly affine transformations.

En los últimos años, la inteligencia robótica esta siendo desarrollada gracias a los últimos avances tecnológicos. A través de la visión por computador, los sistemas inteligentes han sido diseñados para permitir a los robots simular comportamientos autónomos. En este articulo, hemos diseñado un sistema de captura y clasificación de objetos para permitir al Aibo, el robot de Sony, interactuar con su entorno. Los experimentos han mostrado un buen rendimiento reconociendo objetos sintéticos y simulando comportamientos autónomos en entornos no controlados con ruido. A parte, hemos extendido nuestro sistema para trabajar en el reconocimiento de señales de tráfico reales.

Als darrers anys, la intel·ligència robòtica ha estat desenvolupada a partir dels últims avanços tecnológics. Basant-se en els sistemas de visió per computador, els sistemas intel·ligents han estat disenyats per permetre als robots simular comportaments autonoms. En aquest article, hem disenyat un sistema de captura i classificació de objectes per permitir al aibo interactuar amb el seu entorn. Els experiments han mostrat un bon rendimient en el reconeixemente de objectes sintètics i simulació de comportaments autònoms en entorns no controlats amb soroll. A part, hem extès el nostre sistema per treballar al reconeixement de senyals de tràfic reals.

Index

Real-time sign classification for Aibo robots

José Luis Ledesma Piqueras[1]

Abstract

Last years robotics intelligence has shown significant improvement due to the high quality of the actual technology. Based on last advances of Computer Vision, intelligent systems have been designed to allow the robotics devices to simulate autonomous behaviors. In this paper, we design a real-time model matching and classification system in order to allow an Aibo robot to interact with its environment. The experiments show good performance on synthetic objects recognition in cluttered scenes, and simulate autonomous behaviors in non-controlled environments. Besides, we extend our system to run in real traffic sign recognition system. In different real experiments, our application shows a good performance being robust either in case of lack of visibility, partial occlusions, illumination changes and slightly affine transformations.

Index Terms

Robotics, Computer Vision, Model Matching, Multiclass classification, k-NN, Fisher Linear Discriminant Analisys.

[1]José Luis Ledesma Piqueras is a member of the Escuela Técnica Superiot de Ingeniería, UAB, Edifici Q, Campus UAB, Bellaterra, 08193, Spain. E-mail: joseluis.ledesma@gmail.com

I. INTRODUCTION

Robotics deals with the practical application of many artificial intelligence techniques to solve real-world problems. This combines problems of sensing and modelling the world, planning and performing tasks, and interacting with the world. One of the main ways to interact with the environment is throw artificial vision, where the goal is to make useful decisions about real physical objects and scenes based on sensed images. It uses statistical methods to extract data using models based on geometry, physics and learning theory. Vision applications range from mobile robotics, industrial inspection and satellite image understanding, to human computer interaction, image retrieval from digital libraries, medical image analysis, proteinic image analysis and realistic rendering of synthetic scenes in computer graphics.

The Aibo robot from Sony (fig. 1) is a perfect tool to implement and test artificial intelligent techniques in robotics. The AIBO robot combines a body (hardware) and mind (the Aibo Mind 3 software) that allow it to move, think, and display the lifelike attribute of emotion, instinct, learning and growth. It establishes communication with people by displaying emotions, and assumes various behaviors (autonomous actions) based on information which it gathers from its environment. The Aibo robot is not only a robot, but an autonomous robot with the ability to complement your live. While living with you, the behavior of the Aibo robot patterns develops as it learns and grows. Also, it lets you to implement new complex behaviors depending on the environment. So it is the best tool to try and test a signs recognition system in real environments. There is no other so developed technology embedded in a simple but intelligent robot.

Object recognition process basically is composed by three steps: detection of a region of interest (ROI), model matching, and classification. Each of these steps can be done by a great different number of algorithms. Depending on the object we want to recognize, different techniques offer different performance depending on the domain. Adaboost [3] has been at last years one of the most used technique for object detection, feature selection, and object classification. Usually, the problem of object recognition (e.g. person identification) needs a previous addressing the category detection (e.g. face location). According to the way objects are described, three main families of approaches can be considered [12]: part-based, patch-based and region-based methods. Part-based approaches consider that an object is defined as a specific spatial arrangement of the object parts. An unsupervised statistical learning of constellation of parts and spatial relations is used in [10]. In [11] and [13] a representation integrating Boosting with constellations of contextual descriptors is defined, where the feature vector includes the bins that correspond to the different positions of the correlograms determining the object properties. Patch-based methods classify each rectangular image region of a fixed aspect ratio (shape) at multiple sizes, as object (or parts of the target object) or background. In [9], objects are described by the best features obtained using masks and normalized cross-correlation. Finally, region-based algorithms segment regions of the image from the background and describe them by a set of features that provide texture and shape information. In [11], the selection of feature points is based on image contour points. Model matching normally is adapted depending on the domain we are working on, and finally, object classification involves a lot of techniques to solve the problem of discriminability between different types of objects (classes).

Fig. 1. Sony Aibo robot.

When the number of classes to discriminate are higher of two, the multiclass classification is normally generated expending a set of two-class classifiers. The most common classifiers used in the literature are: K-Nearest neighbors, Principal Components Analysis, Fisher Discriminant Analysis, Tangent Distance, Adaboost variants, Support Vector Machine, etc.

In our application, we make use of the results of the Adaboost procedure as a detection algorithm. The use of this algorithm let us detect regions of interest with high probability of containing signs. Once the Adaboost returns a ROI, we fit the model using the circular geometry properties, obtaining the estimated center and the radius of the sign. The main reason of using the circular geometry is the robustness of the algorithm. Once we have fit the model, using k-NN classification method we obtain the label of the sign. We can use safely k-NN with the synthetic signs we have created, because these signs are very different between them. The system is validated in a Sony Aibo robot showing good performance on recognizing objects in real-time. In the next part the methodology to solve a real traffic sign recognition system is shown. All the algorithms used are separately explained. Following one can read about the results of applying the different algorithms.

This paper is organized as follows: Section 1 overviews robotics, artificial vision and introduces the paper goal and scope. Section 2 describes the required techniques of the methodology and it shows the architecture of our proposed system. Section 3 shows the experiments and results, and section 4 concludes the paper.

II. METHODOLOGY

In this chapter, we explain the techniques used to solve the model matching and classification of objects. Finally, we show the integrated strategies in the real application.

A. *Adabost Detection*

The AdaBoost boosting algorithm has become over the last few years a very popular algorithm to use in practice. The main idea of AdaBoost is to assign each example of the given training set a weight. At the beginning all weights are equal, but in every round the weak learner returns a hypothesis, and the weights of all examples classified wrong by that hypothesis are increased. That way the weak learner is forced to focus on the difficult examples of the training set. The final hypothesis is a combination of the hypotheses of all rounds, namely a weighted majority vote, where hypotheses with lower classification error have higher weight. Summarizing, the approach consists of a) choosing a (weak) classifier, b) modifying example weights in order to give priority to examples where the previous classifiers fail, and c) combining classifiers in a multiple classifier. The combined classifier allows a good generalization performance with the only requirement that each weak learner obtains an accuracy better than random [9]. The Adaboost procedure has been used for feature selection, detection, and classification problems. In our problem, the Gentle Adaboost has been previously applied to detect the regions of interest (ROI) with high probability of containing signs from the Aibo video data. In fig. 2 the Gentle Adaboost algorithm of our approach, that has been shown to outperform the other Adaboost versions.

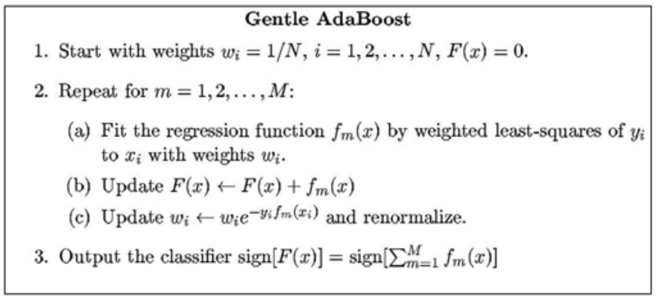

```
Gentle AdaBoost
1. Start with weights $w_i = 1/N$, $i = 1, 2, \dots, N$, $F(x) = 0$.
2. Repeat for $m = 1, 2, \dots, M$:
    (a) Fit the regression function $f_m(x)$ by weighted least-squares of $y_i$
        to $x_i$ with weights $w_i$.
    (b) Update $F(x) \leftarrow F(x) + f_m(x)$
    (c) Update $w_i \leftarrow w_i e^{-y_i f_m(x_i)}$ and renormalize.
3. Output the classifier $\text{sign}[F(x)] = \text{sign}[\sum_{m=1}^{M} f_m(x)]$
```

Fig. 2. Gentle Adaboost algorithm

In fig. 2, the weights of each of the samples of the training set are initialized. Normally, the same weight is assigned to each sample satisfying $\sum_{i=1}^{N} w_i = 1$. At iteration m of the algorithm, a weak classifier evaluates the feature space and selects the best feature based on the weights of the samples. The samples are re-weighted with a exponential loss-function, and the process is repeated M times or when the training classification error is zero. The final strong classifier of the Gentle Adaboost algorithm is an additive model that use a threshold as a final classifier. To classify a new input, the results of applying the m weak classifiers with the test sample are added or subtracted depending on the accuracy of each weak classifier. In the common case of using decision stumps as a weak classifier, the additive model assigns the same weight to each of the hypothesis, so all the features are considered to have the same importance. The last fact is the main difference between the Gentle Adaboost and the traditional Adaboost versions.

Given an Adaboost positive sample, it determines a region of interest (ROI) that contains an object. However, besides the ROI we miss information about scale and position, so before applying recognition we need to apply a spatial normalization. Concerned with the correlation of sign distortion, we look for affine transformations that can perform the spatial normalization to improve final recognition.

B. *Model fitting*

In order to capture the model contained in the detected ROI, we consider the radial properties of the circular signs to fit a possible instance and to estimate its center and radius.

Fast radial symmetry: The fast radial symmetry [4] is calculated over a set of one or more ranges N depending on the scale of the features one is trying to detect. The value of the transform at range indicates the contribution to radial symmetry of the gradients a distance n away from each point. At each range n we define an orientation projection image O_n (1) and (2), generated by examining the gradient g at each point p, from which a corresponding positively-affected pixel $p_{+ve}(p)$ and negatively-affected pixel $p_{-ve}(p)$ are determined (3) and (4).

$$O_n(P_{+ve}(p)) = O_n(P_{+ve}(p)) + 1 \tag{1}$$

$$O_n(P_{-ve}(p)) = O_n(P_{-ve}(p)) + 1 \tag{2}$$

$$P_{+ve}(p) = p + round\frac{g(p)}{||g(p)||}n \tag{3}$$

$$P_{-ve}(p) = p - round\frac{g(p)}{||g(p)||}n \tag{4}$$

Now, to locate the radial symmetry position, we search for the maximum position (x, y) at accumulated orientations matrix O^T:

$$O^T = \sum_{i=1}^{n} O_n \tag{5}$$

Locating that maximum at the respective orientation matrix, we determine the radius length. This procedure allows to obtain robust results for circular traffic signs fitting. An example is shown in fig. 3.

The ROI that contains a circular sign may contain noise inside and outside the object that can slightly displace the center. To cope with this possible displacement, we can iterate this procedure applying a circular mask to exclude near points that can displace the center of the sign, and repeat the process limiting the radius range fig. 4.

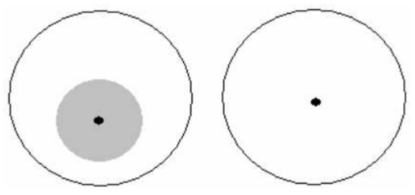
Fig. 4. (a). Displaced center due to noise, and mask to exclude near points of high gradient module. (b) Center correction from the next iteration of radial symmetry.

C. *Classification techniques*

K**-Nearest Neighbors:** Among the various methods of supervised statistical pattern recognition, the Nearest Neighbour rule achieves consistently high performance, without a priori assumptions about the distributions from which the training examples are drawn. It involves a training set of both positive and negative cases. A new sample is classified by calculating the distance to the nearest training case; the sign of that point then determines the classification of the sample. The k-NN classifier extends this idea by taking the k nearest points and assigning the sign of the majority. It is common to select k small and odd to break ties (typically 1, 3 or 5). Larger k values help reduce the effects of noisy points within the training data set, and the choice of k is often performed through cross-validation. In this way, given a input test sample vector of features x of dimension n, we estimate its Euclidean distance d (6) with all the training samples (y) and classify to the class of the minimal distance.

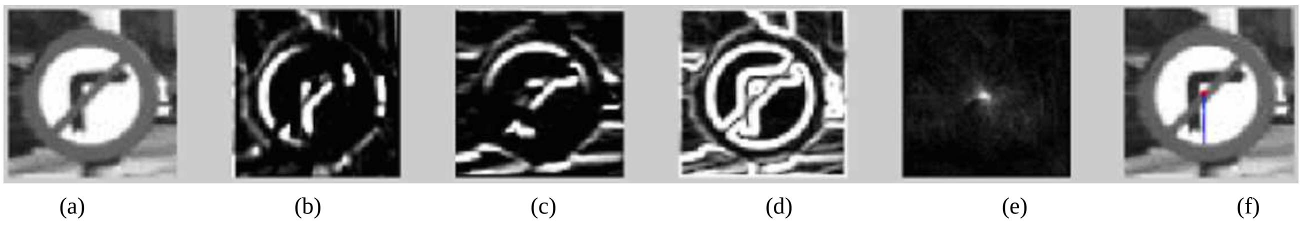

Fig. 3. (a) Input image, (b) X-derived, (c) Y-derived, (d) image gradient g, (e) total orientations accumulator matrix OT, (f) Captured center and radius.

$$d(x,y)=\sqrt{\sum_{j=1}^{n}(x_j-y_j)^2} \tag{6}$$

Principal Components Analysis: Principal Component Analysis, from a statistical perspective, is a method for transforming correlated variables into uncorrelated variables, finding linear combinations of the original variables with relatively large or small variability, as well as for reducing data dimensionality [5].

Given the set of N column vectors $\{\overrightarrow{x}_i\}$ of dimension D, the mean of the data is:

$$\overrightarrow{\mu}_x=\frac{1}{N}\sum_{i=1}^{N}\overrightarrow{x}_i \tag{7}$$

The scatering total matrix is defined as:

$$S_T=\frac{1}{N}\sum_{i=1}^{N}(\overrightarrow{x}_i-\overrightarrow{\mu})(\overrightarrow{x}_i-\overrightarrow{\mu})^T \tag{8}$$

We choose the eigenvectors of S_T that correnpond to the $X\%$ largest eigenvalues of S_T to compute W_{pca}, obtaining a transformation $X^n \mapsto Y^m$, reducing data of the form:

$$Y=W_{pca}(X-\overline{X}) \tag{9}$$

where X is the sample to project and $\overline{X}$ is the data mean.

Fisher Linear Discriminant Analysis(FLDA): Given the binary classification problem, FLDA projects at one dimension each pair of classes (reducing to $C-1$ where C is the number of classes), multiplying each sample by its projection matrix, which minimizes the distance between samples of the same class, and maximizes the distance between the two classes. The result is shown in fig. 5, where the blue and red points belong to the samples of the two projected classes, and the green line indicates the threshold that best separates them [6].

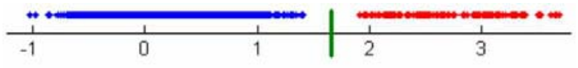

Fig. 5. Fisher projection for two classes and threshold value.

The algorithm is as follows: Given the set of N column vectors $\{\overrightarrow{x}_i\}$ of dimension D, we calculate the mean of the data. For K classes $C_1, C_2, ..., C_K$, the mean of the class C_k that contains N_k elements is:

$$\overrightarrow{\mu}_{xk}=\frac{1}{N_k}\sum_{\overrightarrow{x}_i\in C_k}x_i \tag{10}$$

The separability maximization between classes is defined as the quotient between the between-class scatter matrix:

$$S_B=\sum_{k=1}^{K}(\overrightarrow{\mu}_{xk}-\overrightarrow{\mu}_x)(\overrightarrow{\mu}_{xk}-\overrightarrow{\mu}_x)^T \tag{11}$$

and the intra-class scatter matrix:

$$S_W=\sum_{k=1}^{K}\sum_{\overrightarrow{x}_i\in C_k}(\overrightarrow{x}_i-\overrightarrow{\mu}_{xk})(\overrightarrow{x}_i-\overrightarrow{\mu}_{xk})^T \tag{12}$$

The projection matrix W maximizes:

$$\frac{W^T\times S_B\times W}{W^T\times S_W\times W} \tag{13}$$

Let $\overrightarrow{w}_1, ..., \overrightarrow{w}_D$ be the generalized eigenvectors of S_B and S_W. Then, selecting $d<D$ that corresponds to the highest eigenvalue, we have the projection matrix $W=\overrightarrow{W}_1, ..., \overrightarrow{W}_D$, project the samples to the new space by using:

$$\overrightarrow{y} = W_d^T \overrightarrow{x} \tag{14}$$

The generalized eigenvectors of (12) are the eigenvectors of $S_B S_W^{-1}$.

D. *System*

In this section, we explain the architecture of the whole application after integrating the previous techniques. The scheme of the whole system is shown in fig. 6.

The process starts with the autonomous Aibo robot interaction, the captured frames are processed at the detection step by the Gentle Adaboost Algorithm (see appendix E). The detected ROIs with a high probability of containing a circular sign are sent to our system to proceed with the model fitting and posterior classification. First, fast radial symmetry is applied to the ROI, and if the specifications succeed, the captured region is normalized previously to classify (see results section). At the classification step, $k-NN$ and Fisher Linear Discriminant Analysis with a previous Principal Components Analysis (FLDA) depending on the type of the fitted object is applied.

III. Results

Aibo has a VGA quality camera, which gives a maximum resolution of 640×480. Once the image is captured, and after converting the image to greyscale, the Adaboost algorithm is applied to detect all the ROIs, that are the inputs of our system.

A. *Model matching parameters*

Given an Adaboost image, it determines a region of interest that contains a sign. Still, given the ROI we miss information about the sign scale and position, so before applying recognition we need to apply a spatial normalization. Concerned with the correlation of sign distortion, we look for affine transformations that can perform the spatial normalization to improve final recognition.

First, all the points in the image are treated in the same way. We get the module and the derivative of each point of the image projecting it for different radius values to find the center. These initial radius estimates are from 20% to 50% of the image height. The only procedure we apply in this first step is a simple threshold to try to determine if the point we are working on is part of the boundary of the sign. This threshold is determined by the 10% of the gradient image max value. Once the algorithm is applied for first time, we have the object center and radius, probably affected by the noise of the image.

In order to make a better approximation, a mask over the center of the estimated sign is applied, that avoids the effect of the inner-sign noise. To prevent the possible previous displacement of the containing noise, and to remove the inner-sign noise by means of the mask, instead of using a large number of radius to determine the center, we also limit the number of radius we use. So, in this second time we apply this algorithm we use a radius from 80% to the 120% of the previous calculated radius. In fact, we are using the same algorithm all the time, but limiting the importance of each point in the image, to fit the real center and radius of the sign limiting the center searching and avoiding the effect of the typical noise of real images.

In some cases, the ROIs obtained by the use of the Gentle Adaboost algorithm can be false positives (regions detected with as probability of containing a sign that really corresponds to background regions). Besides to optimize the model fitting, we approximate a new methodology to detect false positives. To avoid this problem, as we know some a priori characteristics about the object representation, we can use that properties to detect false regions. We know that the center of the sign will be more or less at the center of the image, and also that the radius is approximately $2/3$ of the height of the image. In this way, any sign detected that did not match these basic characteristics is a false positive. In this way, the false positives detection is based on estimating the theshold values to avoid false positives based on (eq.15), where $C = (c_x, c_y)$ corresponds to the center position, h and w correspond to the height and width of the ROI, and c_{x_1} and c_{y_1} are the intervals to consider a positive possible estimation of the center for a real sign. For the radius threshold, the restriction is based in obtaining a radius value R between the interval $[0.5\frac{h}{2}, 1.5\frac{h}{2}]$,thus leading to:

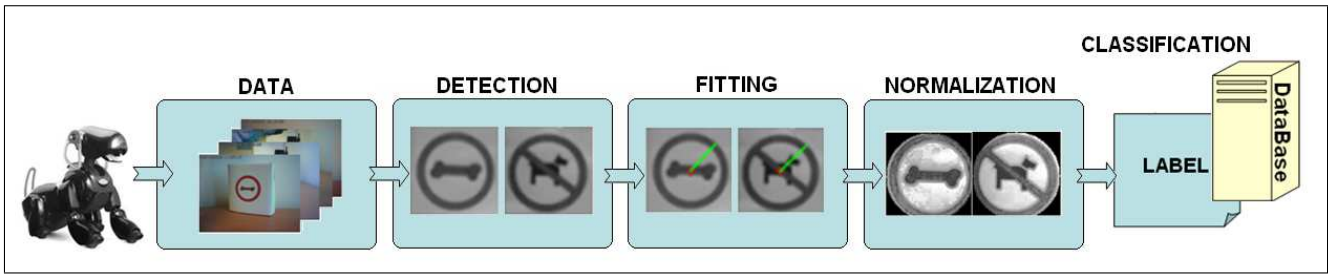

Fig. 6. Whole intelligent Aibo process scheme.

$$c_{y_1} \in [0.6\frac{h}{2}, 1.4\frac{h}{2}], c_{x_1} \in [0.6\frac{x}{2}, 1.4\frac{x}{2}] \quad (15)$$

Once we have a good approximation about the center and the radius of the circular sign, we have to normalize it before classification.

B. *Normalization parameters*

The normalization process consists in four steps. First we rescale it to a 30×30 pixels image. Secondly we equalize the image. When one wishes to compare two or more images on a specific basis, such as texture, it is common to first normalize their histograms to a ”standard” histogram. This can be especially useful when the images have been acquired under different circumstances. The most common histogram normalization technique is histogram equalization where one attempts to change the histogram through the use of a function $b = f(a)$ into a histogram that is constant for all brightness values. This would correspond to a brightness distribution where all values are equally probable. Unfortunately, for an arbitrary image, one can only approximate this result. For a ”suitable” function $f(*)$ the relation between the input probability density function, the output probability density function, and the function $f(*)$ is given by:

$$p_b(b)db = p_a(a)da \quad \Longrightarrow \quad df = \frac{p_a(a)da}{p_b(d)} \quad (16)$$

From (16) we see that ”suitable” means that $f(*)$ is differentiable and that $df/da \geqq 0$. For histogram equalization we desire that $pb(b) = constant$ and this means that:

$$f(a) = (2^B - 1) \times p(a) \quad (17)$$

where $P(a)$ is the probability distribution function. In other words, the quantized probability distribution function normalized from 0 to $2B - 1$ is the look-up table required for histogram equalization. The histogram equalization procedure can also be applied on a regional basis.

The regions of the sign are not homogeneous, so, classification methods could accumulate errors. To solve this problem, we use different anisotropic filters, Perona and Malik [7] and Weickert [8], and we observed that Weickert filter runs better on our images. Anisotropic filtering is a technique designed to sharpen the textures that appear on surfaces. It works by taking multiple bi-linear or tri-linear texture samples for each pixel, which prevents the blurriness that normally results from textures rendered at sharp angles relative to the viewer. The reason these textures appear blurry is because a single pixel on an angled surface covers a large amount of surface area relative to a pixel on a surface viewed straight on. This means that many more texels will lie in the vicinity of the pixel center, and their values need to be taken into account to accurately determine the pixel color. Rather than just sampling the nearest texels to the pixel center, anisotropic filtering takes additional samples along the slope of the surface. The more strongly sloped the surface is, the more samples will be necessary to maintain image fidelity. In general, 16 samples are sufficient to eliminate any visible blurriness on even the most extremely angled surfaces and mask the image to have visible only the part of the ROI we are interested in: the sign. The result is shown in fig. 7.

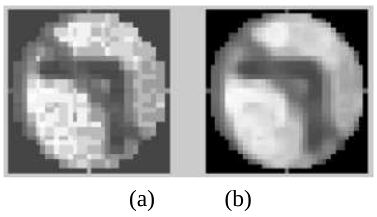

Fig. 7. (a) Extracted equalized sign. (b) Anisotropic Weickert filter.

C. *Database generation*

The database we have used is based on over 500 images of each class, generated and stored using the previous procedures. Much more images will lead to a slower system performance, and less images will reduce the percentage of success. In the k-NN application, a $k = 3$ has obtained a good performance as the number of nearest neighbors considered to classify a given object. The three-class Aibo problem representant are shown in fig. 8.

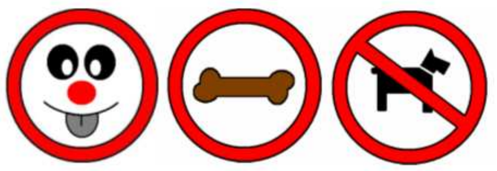

Fig. 8. Aibo circular classes.

D. *Classification parameters*

Now that we have the image normalized, the classification algorithm (k-NN) has to deal with a 3-class to return the sign label.

The k-NN algorithm compares each image it has stored in its database, with the image we have obtained from the model matching. A good database, and a good K election will determine the success of the classification. To determine the real success of the application, each part of it has been accurately tested. For the model matching we have used 500 images, from which the system has returned a 97.4% of success. Whilst the system, at first sight, should return a 100% success, some images are difficult to treat, even for the human eye, as we can see in the fig. 9.

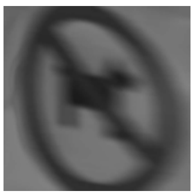

Fig. 9. Difficult captured sign.

The image of fig. 9 shows a difficult image to well-recognize due to the real behavior of Aibo in non-controlled environments. In order to test the classification, we used a ten-fold cross-validation, with a confidence range of 99% interval. We have gotten over 1000 images, and 10 groups of 100 images were made. We use 9 of these groups to train the classification system, and the other one to test it, and we repeated this process ten times. Once we have done the 10 validations, we obtained a 96.2±1.02% average. We calculate the confidence interval by:

$$R = 1.96 \times \frac{std(P)}{\frac{1}{n}\sum_{j=1}^{n} P(j)} \tag{18}$$

where P is the vector with the n classification iterations, R is the confidence interval, and std is the standard deviation. After this test, we obtained that the whole system has a performance of 93.69% success, which, up to our opinion, is highly robust taking in to account that the application is running in a non-controlled environments. In fig. 10 a process of a synthetic Aibo image to fit the model is shown, and fig. 11 shows the normalized image.

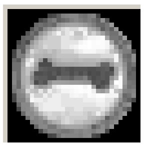

Fig. 11. Normalized-rescaled Aibo recognized sign.

E. *Real traffic sign recognition system*

In order to test the robustness of our system in real application, we have applied it to a real traffic sign recognition system. This test allowed us not only to work in a real non-controlled system, but also to work with real objects (non synthetic ones as in the previous case) that can appear in different conditions, and with different appearance. In this

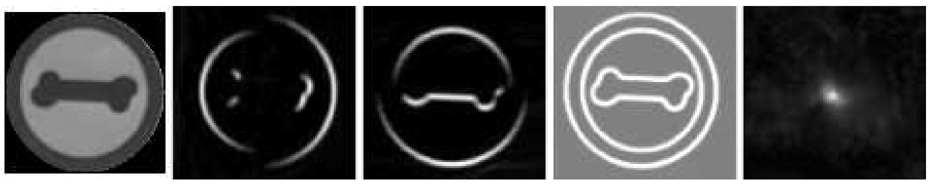

Fig. 10. Synthetic image fitting.

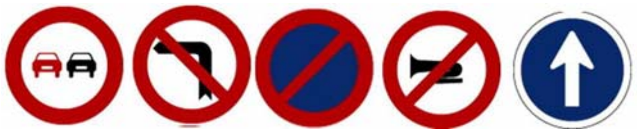

Fig. 12. Real traffic sign circular classes.

Fig. 13. Real traffic sign speed classes.

way, a new problem is introduced: not all the objects are enough discriminable and some of them share similar features, so it is more difficult to obtain a high recognition performance. In fig. 12 and 13, the different classes of speed signs are shown. Each speed sign is very close to the others, that makes more difficult the work of k-NN since slight movements can introduces high correlation errors. We have also used FLDA (with a previous 99.99% of PCA) to obtain a more sophisticated classification comparative since FLDA is known to work with a data projection with a previous training that estimate a matrix projection that optimally split the samples. FLDA is a one-versus-one class algorithm, so we have used a pairwise voting system, to extend the FLDA as a binary classifier to a multiclass problem. The voting scheme (pairwise) uses a matrix of dimension $N_c \times N_c$, where N_c is the number of classes. Each position for a test input sample corresponds to the class with a high membership probability using classifier that trains class of row i versus class of column j. In this way, in the final tested matrix the maximal voting value for a class corresponds to the classification label.

The circular group is treated in the same way that the synthetic Aibo images. For the speed group we applied a normalization strategy. As the speed group does not have intermediate level of greys levels, it is better to binarize the regions to avoid the error that can be accumulated by false grey levels that can appear due to different conditions as shadows. In fig. 15 different signs extracted from 1024$\times$1024 real images at different real conditions are shown to observe the difficulty to classify in these adverse conditions.

In this way, when we receive a ROI from the Adaboost procedure obtained by the training of real images, the ROI is fitted with the optimized fast radial symmetry, and classified. In case to be classified by the speed group (with a class that contains all the speed classes together), a new classification is done with a new binary database of speed classes with the two different classification strategies. Fig. 14 shows the new scheme adapted to the real sign recognition system, where one can see the different treatment when a speed sign is classified. The data used for this test is a set of 200 real samples for the circular group and the same number of samples for the real speed classes.

As we can see in the table I, k-NN and FLDA are very near in success where we are treating with well-discriminate classes, although in this case FLDA allow us to classify more quickly by the fact that we only need a multiplication and threshold comparison instead to compare with all the stored images of the database classes. When we are working with very similar classes, the k-NN algorithm looses a lot of precision, meanwhile FLDA treated with them with a great success, as the results and confidence

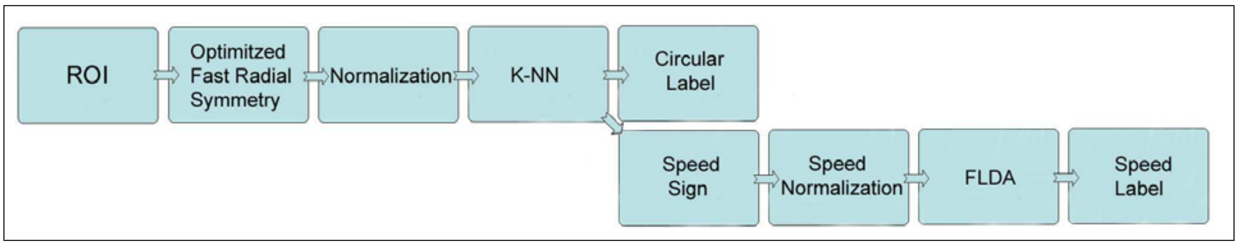

Fig. 14. Real traffic sign system scheme.

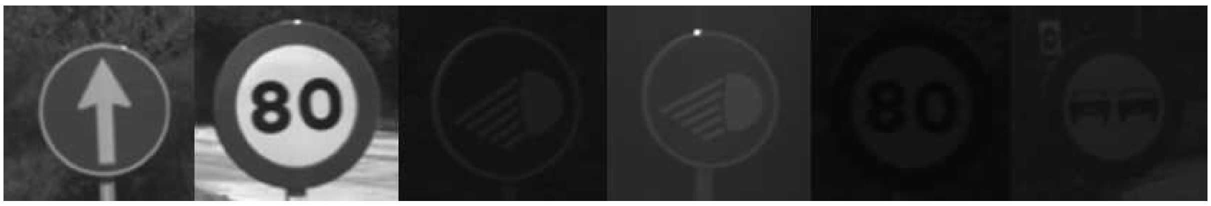

Fig. 15. Different ROIs of real traffic sign at different real conditions.

	Circular group	Speed group
k-NN	92.73±1.02	71.14±1.70
FLDA	93.12±0.13	**87.18±1.30**

TABLE I
CLASSIFICATION RESULTS FOR k-NN AND FLDA FOR THE REAL TRAFFIC SIGN GROUPS.

intervals show. The results are also graphically showed in fig. 18 and 19.

F. *Discussion*

In this chapter, we have exposed two different types of experiments. First, the performance for the detection, model matching and classification of the Sony Aibo robot has been shown. The system shows high accuracy with the generated synthetic objects in real non-controlled environments. The k-NN classification technique is a good option due to the high discriminability between classes. The databases do not need aN excessive number of classes and the real-time performance is allowed.

The second experiment is a real validation of the application in a real traffic sign recognition system. This experiment has been done in order to validate the performance of our approaches in environments with difficult conditions to treat. The signs to recognize are less discriminable and they appear in adverse conditions. We have observed that the speed classes require a concrete pre-process to improve the classification step. Due to the low performance of the k-NN strategy at the speed classes, new classification techniques have been required to increase the performance of the process. We have used Fisher Linear Discriminant Analysis with a previous Principal Components Analysis to not use the local-behavior of the k-NN correlation scheme. The projection allowed by FLDA allow us to increase the performance and obtain robust results. In fig. 16 an example of a whole traffic sign captured image and the region of interest that contains a circular sign are shown, and the fig. 17 shows an example of the execution of our process in the Aibo system, where an interface shows the frame captured by the image and the recognized sign.

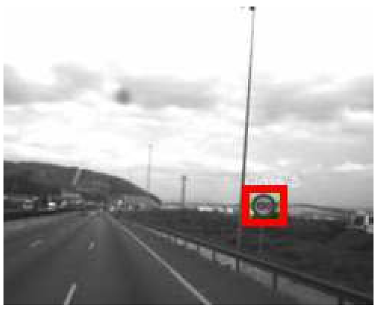

Fig. 16. Real traffic sign image.

IV. CONCLUSIONS

Recently, intelligent robotics and computer vision have shown significant advances. Normally, the design depends on a concrete problem domain. The Sony Aibo robot is a useful robotic tool to test developed systems on real environments. In this paper, we

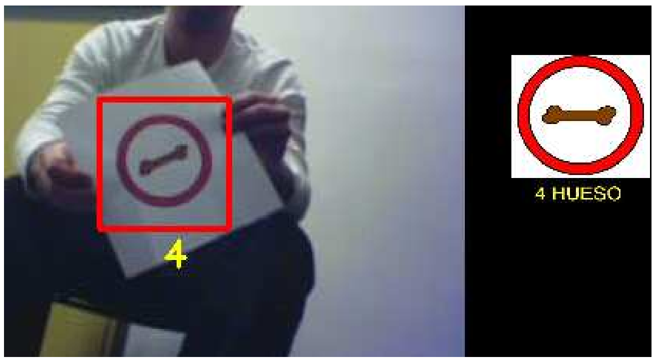

Fig. 17. Aibo system interaction and recognition interface.

have designed a real application to make Aibo recognize synthetic circular objects in cluttered scenes. We developed a robust system to solve the problem of model matching and object classification. The first approach includes well-differentiated synthetic objects, where Aibo shows a high recognition and autonomous behavior performance. After that, we extended the use of the system in a real traffic sign recognition process, proving the robustness of the system recognizing different types of traffic signs at different non-controlled conditions, showing the flexibility and robustness of our application either in case of lack of visibility, partial occlusions, noise, and slight affine transformations.

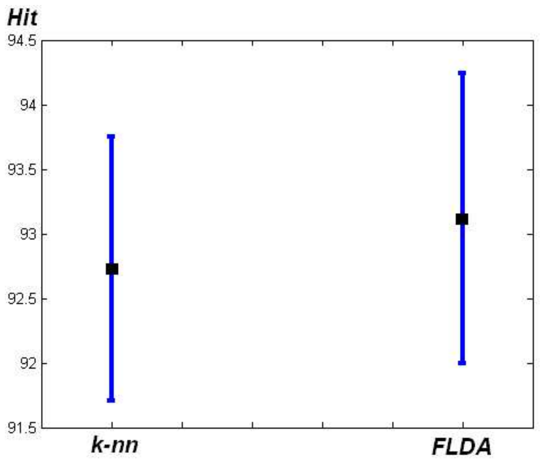

Fig. 18. Classification accuracy for the real circular group using k-NN and FLDA.

V. ACKNOWLEDGEMENTS

I want to acknowledge Sergio Escalera and Petia Radeva the direction in this project. It would not have been possible to develop the project without them. I want to acknowledge the essencial aportation of Xavi, Carlos and Raul. I want also to acknowledge my parents and family for helping me, not only during the realization of this project, but also in my general life. I would also acknowledge all my friends that have stand me in the worst moments, with a very special mention to Sergio, Tania, Annita, Dunia and Gomez. Thanks for being near me always I need you.

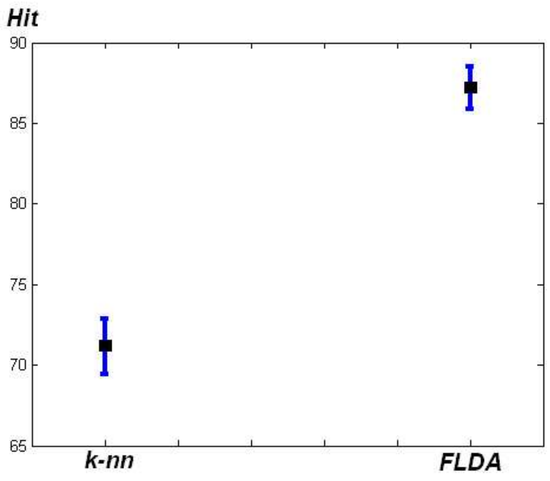

Fig. 19. Classification accuracy for the real speed group using k-NN and FLDA.

REFERENCES

[1] Yoav Freund and Robert E. Schapire. ”A decision-theoretic generalization online learning and an application to boosting,” Computational Learning Theory: Eurocolt ’95, pages 23-37. Springer-Verlag, 1995.
[2] Paul Viola and Michael J. Jones, ”Robust Real-time Object Detection,” Cambridge Research Laboratory, Technical Report Series, CRL 2001/01. Feb. 2001.
[3] J. Friedman, T. Hastie, and R. Tibshirani, ”Additive logistic regression: a statistical view of boosting”, Technical Report, 1998.
[4] G. Loy, and A. Zelinsky, ”A Fast Radial Symmetry Transform for Detecting Points of Interest”, Transactions on PAMI, 2003.
[5] Lindsay I Smith , ”A tutorial on Principal Components Analysis”, February, 2002
[6] MaxWelling , ”Fisher Linear Discriminant Analysis”, Department of Computer Science, University of Toronto, 2002.
[7] Perona P., Malik J., ”Scale space and edge detection using anisotropic diffusion”, IEEE Trans. Pattern Anal. Machine Intell., Vol. 12, pp. 629-639, July 1990.
[8] Weickert J., ”Anisotropic diffusion in image processing”, European Consortium for Mathematics in Industry (B.G. Teubner,Stuttgart), 1998.
[9] A. Torralba, K. Murphy and W. Freeman, ”Sharing Visual Features for Multiclass and Multiview Object Detection”, CVPR, pp. 762-769, vol. 2, 2004.
[10] R. Fergus, P. Perona, and A. Zisserman, ”Object class recognition by unsupervised scale-invariant learning”, CVPR, 2003.
[11] J. Amores, N. Sebe and P. Radeva, ”Fast Spatial Pattern Discovery Integrating Boosting with Constellations of Contextual Descriptors”, CVPR, 2005.
[12] K. Murphy, A.Torralba and W.T.Freeman, ”Using the Forest to See the Trees: A Graphical Model Relating Features, Objects, and Scenes”, Advances in NIPS, MIT Press, 2003.
[13] S. Escalera, O. Pujol, and P. Radeva, ”Boosted Landmarks of contextual descriptors and Forest-ECOC: A novel framework to detect and classify objects in cluttered scenes”, International Conference on Pattern Recognition, Hong Kong, 2006.

Appendices

To complement the information of the project that can not be included in the article, some appendices have been included. In order to explain in more detail the domain of the work, first appendix is related to the Artificial Intelligence History. In the topic of Artificial Intelligence, we have basically focused on Artificial Vision, so the next appendix is an overview of Computer Vision. The following two appendices explain the origin of the real traffic sign data that we process in this work, and the technics specifications of the Sony Aibo robot as the autonomous system used in the project. Finally, the source code of the application is shown.

Appendix A. Artificial Intelligence history

Prehistory of AI

Humans have always speculated about the nature of mind, thought, and language, and searched for discrete representations of their knowledge. Aristotle tried to formalize this speculation by means of syllogistic logic, which remains one of the key strategies of AI. The first is-a hierarchy was created in 260 by Porphyry of Tyros. Classical and medieval grammarians explored more subtle features of language that Aristotle shortchanged, and mathematician Bernard Bolzano made the first modern attempt to formalize semantics in 1837.

Early computer design was driven mainly by the complex mathematics needed to target weapons accurately, with analog feedback devices inspiring an ideal of cybernetics. The expression "artificial intelligence" was introduced as a 'digital' replacement for the analog 'cybernetics'.

Development of AI theory

Much of the (original) focus of artificial intelligence research draws from an experimental approach to psychology, and emphasizes what may be called linguistic intelligence (best exemplified in the Turing test).

Approaches to Artificial Intelligence that do not focus on linguistic intelligence include robotics and collective intelligence approaches, which focus on active manipulation of an environment, or consensus decision making, and draw from biology and political science when seeking models of how "intelligent" behavior is organized.

AI also draws from animal studies, in particular with insects, which are easier to emulate as robots (see artificial life), as well as animals with more complex cognition, including apes, who resemble humans in many ways but have less developed capacities for planning and cognition. Some researchers argue that animals, which are apparently simpler than humans, ought to be considerably easier to mimic. But satisfactory computational models for animal intelligence are not available.

Seminal papers advancing AI include "A Logical Calculus of the Ideas Immanent in Nervous Activity" (1943), by Warren McCulloch and Walter Pitts, and "On Computing Machinery and Intelligence" (1950), by Alan Turing, and "Man-Computer Symbiosis" by J.C.R. Licklider. See Cybernetics and Turing test for further discussion.

There were also early papers which denied the possibility of machine intelligence on logical or philosophical grounds such as "Minds, Machines and Gödel" (1961) by John Lucas.

With the development of practical techniques based on AI research, advocates of

AI have argued that opponents of AI have repeatedly changed their position on tasks such as computer chess or speech recognition that were previously regarded as "intelligent" in order to deny the accomplishments of AI. Douglas Hofstadter, in Gödel, Escher, Bach, pointed out that this moving of the goalposts effectively defines "intelligence" as "whatever humans can do that machines cannot".

John von Neumann (quoted by E.T. Jaynes) anticipated this in 1948 by saying, in response to a comment at a lecture that it was impossible for a machine to think: "You insist that there is something a machine cannot do. If you will tell me precisely what it is that a machine cannot do, then I can always make a machine which will do just that!". Von Neumann was presumably alluding to the Church-Turing thesis which states that any effective procedure can be simulated by a (generalized) computer.

In 1969 McCarthy and Hayes started the discussion about the frame problem with their essay, "Some Philosophical Problems from the Standpoint of Artificial Intelligence".

Experimental AI research

Artificial intelligence began as an experimental field in the 1950s with such pioneers as Allen Newell and Herbert Simon, who founded the first artificial intelligence laboratory at Carnegie Mellon University, and John McCarthy and Marvin Minsky, who founded the MIT AI Lab in 1959. They all attended the Dartmouth College summer AI conference in 1956, which was organized by McCarthy, Minsky, Nathan Rochester of IBM and Claude Shannon.

Historically, there are two broad styles of AI research - the "neats" and "scruffies". "Neat", classical or symbolic AI research, in general, involves symbolic manipulation of abstract concepts, and is the methodology used in most expert systems. Parallel to this are the "scruffy", or "connectionist", approaches, of which artificial neural networks are the best-known example, which try to "evolve" intelligence through building systems and then improving them through some automatic process rather than systematically designing something to complete the task. Both approaches appeared very early in AI history. Throughout the 1960s and 1970s scruffy approaches were pushed to the background, but interest was regained in the 1980s when the limitations of the "neat" approaches of the time became clearer. However, it has become clear that contemporary methods using both broad approaches have severe limitations.

Artificial intelligence research was very heavily funded in the 1980s by the Defense Advanced Research Projects Agency in the United States and by the fifth generation computer systems project in Japan. The failure of the work funded at the time to produce immediate results, despite the grandiose promises of some AI practitioners, led to correspondingly large cutbacks in funding by government agencies in the late 1980s, leading to a general downturn in activity in the field known as AI winter. Over the following decade, many AI researchers moved into related areas with more modest goals such as machine learning, robotics, and computer vision, though research in pure AI continued at reduced levels.

Micro-World AI

The real world is full of distracting and obscuring detail: generally science progresses by focusing on artificially simple models of reality (in physics, frictionless planes and perfectly rigid bodies, for example). In 1970 Marvin Minsky and Seymour Papert, of the MIT AI Laboratory, proposed that AI research should likewise focus on developing programs capable of intelligent behaviour in artificially simple situations known as micro-worlds. Much research has focused on the so-called blocks world, which consists of coloured blocks of various shapes and sizes arrayed on a flat surface. Micro-World AI

Spinoffs

Whilst progress towards the ultimate goal of human-like intelligence has been slow, many spinoffs have come in the process. Notable examples include the languages LISP and Prolog, which were invented for AI research but are now used for non-AI tasks. Hacker culture first sprang from AI laboratories, in particular the MIT AI Lab, home at various times to such luminaries as John McCarthy, Marvin Minsky, Seymour Papert (who developed Logo there) and Terry Winograd (who abandoned AI after developing SHRDLU).

AI languages and programming styles

AI research has led to many advances in programming languages including the first list processing language by Allen Newell et. al., Lisp dialects, Planner, Actors, the Scientific Community Metaphor, production systems, and rule-based languages.

GOFAI TEST research is often done in programming languages such as Prolog or Lisp. Bayesian work often uses Matlab or Lush (a numerical dialect of Lisp). These languages include many specialist probabilistic libraries. Real-life and especially real-time systems are likely to use C++. AI programmers are often academics and emphasise rapid development and prototyping rather than bulletproof software engineering practices, hence the use of interpreted languages to empower rapid command-line testing and experimentation.

The most basic AI program is a single If-Then statement, such as "If A, then B." If you type an 'A' letter, the computer will show you a 'B' letter. Basically, you are teaching a computer to do a task. You input one thing, and the computer responds with something you told it to do or say. All programs have If-Then logic. A more complex example is if you type in "Hello.", and the computer responds "How are you today?" This response is not the computer's own thought, but rather a line you wrote into the program before. Whenever you type in "Hello.", the computer always responds "How are you today?". It seems as if the computer is alive and thinking to the casual observer, but actually it is an automated response. AI is often a long series of If-Then (or Cause and Effect) statements.

A randomizer can be added to this. The randomizer creates two or more response paths. For example, if you type "Hello", the computer may respond with "How are you today?" or "Nice weather" or "Would you like to play a game?" Three responses (or 'thens') are now possible instead of one. There is an equal chance that any one of the three responses will show. This is similar to a pull-cord talking doll that can respond with a number of sayings. A computer AI program can have thousands of responses to the same input. This makes it less predictable and closer to how a real person would respond, arguably because living people respond somewhat unpredictably. When thousands of input ("if") are written in (not just "Hello.") and thousands of responses ("then") are written into the AI program, then the computer can talk (or type) with most people, if those people know the If statement input lines to type.

Many games, like chess and strategy games, use action responses instead of typed responses, so that players can play against the computer. Robots with AI brains would use If-Then statements and randomizers to make decisions and speak. However, the input may be a sensed object in front of the robot instead of a "Hello." line, and the response may be to pick up the object instead of a response line.

Chronological History

Historical Antecedents

Greek myths of Hephaestus and Pygmalion incorporate the idea of intelligent robots. In the 5th century BC, Aristotle invented syllogistic logic, the first formal deductive reasoning system.

Ramon Llull, Spanish theologian, invented paper "machines" for discovering non-mathematical truths through combinattions of words from lists in the 13th century.

By the 15th century and 16th century, clocks, the first modern measuring machines, were first produced using lathes. Clockmakers extended their craft to creating mechanical animals and other novelties. Rabbi Judah Loew ben Bezalel of Prague is said to have invented the Golem, a clay man brought to life (1580).

Early in the 17th century, René Descartes proposed that bodies of animals are nothing more than complex machines. Many other 17th century thinkers offered variations and elaborations of Cartesian mechanism. Thomas Hobbes published Leviathan, containing a material and combinatorial theory of thinking. Blaise Pascal created the second mechanical and first digital calculating machine (1642). Gottfried Leibniz improved Pascal's machine, making the Stepped Reckoner to do multiplication and division (1673) and evisioned a universal calculus of reasoning (Alphabet of human thought) by which arguments could be decided mechanically.

The 18th century saw a profusion of mechanical toys, including the celebrated mechanical duck of Jacques de Vaucanson and Wolfgang von Kempelen's phony chess-playing automaton, The Turk (1769).

Mary Shelley published the story of Frankenstein; or the Modern Prometheus (1818).

19th and Early 20th Century

George Boole developed a binary algebra (Boolean algebra) representing (some) "laws of thought." Charles Babbage and Ada Lovelace worked on programmable mechanical calculating machines.

In the first years of the 20th century Bertrand Russell and Alfred North Whitehead published Principia Mathematica, which revolutionized formal logic. Russell, Ludwig Wittgenstein, and Rudolf Carnap lead philosophy into logical analysis of knowledge. Karel Capek's play R.U.R. (Rossum's Universal Robots)) opens in London (1923). This is the first use of the word "robot" in English.

Mid 20th century and Early AI

Warren Sturgis McCulloch and Walter Pitts publish "A Logical Calculus of the Ideas Immanent in Nervous Activity" (1943), laying foundations for artificial neural networks. Arturo Rosenblueth, Norbert Wiener and Julian Bigelow coin the term "cybernetics" in a 1943 paper. Wiener's popular book by that name published in 1948. Vannevar Bush published As We May Think (The Atlantic Monthly, July 1945) a prescient vision of the future in which computers assist humans in many activities.

The man widely acknowledged as the father of computer science, Alan Turing, published "Computing Machinery and Intelligence" (1950) which introduced the Turing test as a way of operationalizing a test of intelligent behavior. Claude Shannon published a detailed analysis of chess playing as search (1950). Isaac Asimov published his Three Laws of Robotics (1950).

1956: John McCarthy coined the term "artificial intelligence" as the topic of the Dartmouth Conference, the first conference devoted to the subject.

Demonstration of the first running AI program, the Logic Theorist (LT) written by Allen Newell, J.C. Shaw and Herbert Simon (Carnegie Institute of Technology, now Carnegie Mellon University).

1957: The General Problem Solver (GPS) demonstrated by Newell, Shaw and Simon.

1952-1962: Arthur Samuel (IBM) wrote the first game-playing program, for checkers (draughts), to achieve sufficient skill to challenge a world champion. Samuel's machine learning programs were responsible for the high performance of the checkers player.

1958: John McCarthy (Massachusetts Institute of Technology or MIT) invented the Lisp programming language. Herb Gelernter and Nathan Rochester (IBM) described a theorem prover in geometry that exploits a semantic model of the domain in the form of diagrams of "typical" cases. Teddington Conference on the Mechanization of Thought Processes was held in the UK and among the papers presented were John McCarthy's Programs with Common Sense, Oliver Selfridge's Pandemonium, and Marvin Minsky's Some Methods of Heuristic Programming and Artificial Intelligence.

Late 1950s and early 1960s: Margaret Masterman and colleagues at University of Cambridge design semantic nets for machine translation.

1961: James Slagle (PhD dissertation, MIT) wrote (in Lisp) the first symbolic integration program, SAINT, which solved calculus problems at the college freshman level.

1962: First industrial robot company, Unimation, founded.

1963: Thomas Evans' program, ANALOGY, written as part of his PhD work at MIT, demonstrated that computers can solve the same analogy problems as are given on IQ tests. Edward Feigenbaum and Julian Feldman published Computers and Thought, the first collection of articles about artificial intelligence.

1964: Danny Bobrow's dissertation at MIT (technical report #1 from MIT's AI group, Project MAC), shows that computers can understand natural language well enough to solve algebra word problems correctly. Bert Raphael's MIT dissertation on the SIR program demonstrates the power of a logical representation of knowledge for question-answering systems.

1965: J. Alan Robinson invented a mechanical proof procedure, the Resolution Method, which allowed programs to work efficiently with formal logic as a representation language. Joseph Weizenbaum (MIT) built ELIZA (program), an interactive program that carries on a dialogue in English language on any topic. It was a popular toy at AI centers on the ARPANET when a version that "simulated" the dialogue of a psychotherapist was programmed.

1966: Ross Quillian (PhD dissertation, Carnegie Inst. of Technology, now CMU) demonstrated semantic nets. First Machine Intelligence workshop at Edinburgh: the first of an influential annual series organized by Donald Michie and others. Negative report on machine translation kills much work in Natural language processing (NLP) for many years.

1967: Dendral program (Edward Feigenbaum, Joshua Lederberg, Bruce Buchanan, Georgia Sutherland at Stanford University) demonstrated to interpret mass spectra on organic chemical compounds. First successful knowledge-based program for scientific reasoning. Joel Moses (PhD work at MIT) demonstrated the power of symbolic reasoning for integration problems in the Macsyma program. First successful knowledge-based program in mathematics. Richard Greenblatt (programmer) at MIT built a knowledge-based chess-playing program, MacHack, that was good enough to achieve a class-C rating in tournament play.

1968: Marvin Minsky and Seymour Papert publish Perceptrons, demonstrating limits of simple neural nets.

1969: Stanford Research Institute (SRI): Shakey the Robot, demonstrated combining animal locomotion, perception and problem solving. Roger Schank (Stanford) defined conceptual dependency model for natural language understanding. Later developed (in PhD dissertations at Yale University) for use in story understanding by Robert Wilensky and Wendy Lehnert, and for use in understanding memory by Janet Kolodner. Yorick Wilks (Stanford) developed the semantic coherence view of language called Preference Semantics, embodied in the first semantics-driven machine translation program, and the basis of many PhD dissertations since such as Bran Boguraev and David Carter at Cambridge. First International Joint Conference on Artificial Intelligence (IJCAI) held at Stanford.

1970: Jaime Carbonell (Sr.) developed SCHOLAR, an interactive program for computer assisted instruction based on semantic nets as the representation of knowledge. Bill Woods described Augmented Transition Networks (ATN's) as a representation for natural language understanding. Patrick Winston's PhD program, ARCH, at MIT learned concepts from examples in the world of children's blocks.

Early 70's: Jane Robinson and Don Walker established an influential Natural Language Processing group at SRI.

1971: Terry Winograd's PhD thesis (MIT) demonstrated the ability of computers to understand English sentences in a restricted world of children's blocks, in a coupling of his language understanding program, SHRDLU, with a robot arm that carried out instructions typed in English.

1972: Prolog programming language developed by Alain Colmerauer.

1973: The Assembly Robotics Group at University of Edinburgh builds Freddy Robot, capable of using visual perception to locate and assemble models. The Lighthill report gives a largely negative verdict on AI research in Great Britain and forms the basis for the decision by the British government to discontine support for AI research in all but two universities.

1974: Ted Shortliffe's PhD dissertation on the MYCIN program (Stanford) demonstrated the power of rule-based systems for knowledge representation and inference in the domain of medical diagnosis and therapy. Sometimes called the first expert system. Earl Sacerdoti developed one of the first planning programs, ABSTRIPS, and developed techniques of hierarchical planning.

1975: Marvin Minsky published his widely-read and influential article on Frames as a representation of knowledge, in which many ideas about schemas and semantic links are brought together. The Meta-Dendral learning program produced new results in chemistry (some rules of mass spectrometry) the first scientific discoveries by a computer to be published in a referreed journal.

Mid 70's: Barbara Grosz (SRI) established limits to traditional AI approaches to discourse modeling. Subsequent work by Grosz, Bonnie Webber and Candace Sidner developed the notion of "centering", used in establishing focus of discourse and anaphoric references in NLP. David Marr and MIT colleagues describe the "primal sketch" and its role in visual perception.

1976: Douglas Lenat's AM program (Stanford PhD dissertation) demonstrated the discovery model (loosely-guided search for interesting conjectures). Randall Davis demonstrated the power of meta-level reasoning in his PhD dissertation at Stanford.

Late 70's: Stanford's SUMEX-AIM resource, headed by Ed Feigenbaum and Joshua Lederberg, demonstrates the power of the ARPAnet for scientific collaboration.

1978: Tom Mitchell, at Stanford, invented the concept of Version Spaces for describing the search space of a concept formation program. Herbert Simon wins the Nobel Prize in Economics for his theory of bounded rationality, one of the cornerstones of AI known as "satisficing". The MOLGEN program, written at Stanford by Mark Stefik and Peter Friedland, demonstrated that an object-oriented programming representation of knowledge can be used to plan gene-cloning experiments.

1979: Bill VanMelle's PhD dissertation at Stanford demonstrated the generality of MYCIN's representation of knowledge and style of reasoning in his EMYCIN program, the model for many commercial expert system "shells". Jack Myers and Harry Pople at University of Pittsburgh developed INTERNIST, a knowledge-based medical diagnosis program based on Dr. Myers' clinical knowledge. Cordell Green, David Barstow, Elaine Kant and others at Stanford demonstrated the CHI system for automatic programming. The Stanford Cart, built by Hans Moravec, becomes the first computer-controlled, autonomous vehicle when it successfully traverses a chair-filled room and circumnavigates the Stanford AI Lab. Drew McDermott and Jon Doyle at MIT, and John McCarthy at Stanford begin publishing work on non-monotonic logics and formal aspects of truth maintenance.

1980s: Lisp machines developed and marketed. First expert system shells and commercial applications.

1980: Lee Erman, Rick Hayes-Roth, Victor Lesser and Raj Reddy published the first description of the blackboard model, as the framework for the HEARSAY-II speech understanding system. First National Conference of the American Association for Artificial Intelligence (AAAI) held at Stanford.

1981: Danny Hillis designs the connection machine, a massively parallel architecture that brings new power to AI, and to computation in general. (Later founds Thinking Machines, Inc.)

1982: The Fifth Generation Computer Systems project (FGCS), an initiative by Japan's Ministry of International Trade and Industry, begun in 1982, to create a "fifth generation computer" (see history of computing hardware) which was supposed to perform much calculation utilizing massive parallelism.

1983: John Laird and Paul Rosenbloom, working with Allen Newell, complete CMU dissertations on Soar (program). James F. Allen invents the Interval Calculus, the first widely used formalization of temporal events.

Mid 80's: Neural Networks become widely used with the Backpropagation algorithm (first described by Paul Werbos in 1974).

1985: The autonomous drawing program, AARON, created by Harold Cohen, is demonstrated at the AAAI National Conference (based on more than a decade of work, and with subsequent work showing major developments).

1987: Marvin Minsky publishes The Society of Mind, a theoretical description of the mind as a collection of cooperating agents.

1989: Dean Pomerleau at CMU creates ALVINN (An Autonomous Land Vehicle in a Neural Network), which grew into the system that drove a car coast-to-coast under computer control for all but about 50 of the 2850 miles.

1990s: Major advances in all areas of AI, with significant demonstrations in machine learning, intelligent tutoring, case-based reasoning, multi-agent planning, scheduling, uncertain reasoning, data mining, natural language understanding and translation, vision, virtual reality, games, and other topics. Rodney Brooks' MIT Cog project, with numerous collaborators, makes significant progress in building a humanoid robot.

Early 90's: TD-Gammon, a backgammon program written by Gerry Tesauro, demonstrates that reinforcement (learning) is powerful enough to create a championship-level game-playing program by competing favorably with world-class players.

1997: The Deep Blue chess program (IBM) beats the world chess champion, Garry Kasparov, in a widely followed match. First official RoboCup football (soccer) match featuring table-top matches with 40 teams of interacting robots and over 5000 spectators.

1998: Tim Berners-Lee published his Semantic Web Road map paper [2].

Late 90's: Web crawlers and other AI-based information extraction programs become essential in widespread use of the World Wide Web. Demonstration of an Intelligent room and Emotional Agents at MIT's AI Lab. Initiation of work on the Oxygen architecture, which connects mobile and stationary computers in an adaptive network.

2000: Interactive robopets (”smart toys”) become commercially available, realizing the vision of the 18th century novelty toy makers. Cynthia Breazeal at MIT publishes her dissertation on Sociable machines, describing Kismet (robot), with a face that expresses emotions. The Nomad robot explores remote regions of Antarctica looking for meteorite samples.

2004: OWL Web Ontology Language W3C Recommendation (10 February 2004).

Appendix B. Computer Vision

The field of computer vision can be characterized as immature and diverse. Even though earlier work exists, it was not until the late 1970's that a more focused study of the field started when computers could manage the processing of large data sets such as images. However, these studies usually originated from various other fields, and consequently there is no standard formulation of the "computer vision problem". Also, and to an even larger extent, there is no standard formulation of how computer vision problems should be solved. Instead, there exists an abundance of methods for solving various well-defined computer vision tasks, where the methods often are very task specific and seldom can be generalized over a wide range of applications. Many of the methods and applications are still in the state of basic research, but more and more methods have found their way into commercial products, where they often constitute a part of a larger system which can solve complex tasks (e.g., in the area of medical images, or quality control and measurements in industrial processes).

Computer vision is by some seen as a subfield of artificial intelligence where image data is being fed into a system as an alternative to text based input for controlling the behaviour of a system. Some of the learning methods which are used in computer vision are based on learning techniques developed within artificial intelligence.

Since a camera can be seen as a light sensor, there are various methods in computer vision based on correspondences between a physical phenomenon related to light and images of that phenomenon. For example, it is possible to extract information about motion in fluids and about waves by analyzing images of these phenomena. Also, a subfield within computer vision deals with the physical process which given a scene of objects, light sources, and camera lenses forms the image in a camera. Consequently, computer vision can also be seen as an extension of physics.

A third field which plays an important role is neurobiology, specifically the study of the biological vision system. Over the last century, there has been an extensive study of eyes, neurons, and the brain structures devoted to processing of visual stimuli in both humans and various animals. This has led to a coarse, yet complicated, description of how "real" vision systems operate in order to solve certain vision related tasks. These results have led to a subfield within computer vision where artificial systems are designed to mimic the processing and behaviour of biological systems, at different levels of complexity. Also, some of the learning-based methods developed within computer vision have their background in biology.

Yet another field related to computer vision is signal processing. Many existing methods for processing of one-variable signals, typically temporal signals, can be extended in a natural way to processing of two-variable signals or multi-variable signals in computer vision. However, because of the specific nature of images there are many methods developed within computer vision which have no counterpart in the processing of one-variable signals. A distinct character of these methods is the fact that they are non-linear which, together with the multi-dimensionality of the signal, defines a subfield in signal processing as a part of computer vision.

Beside the above mentioned views on computer vision, many of the related research topics can also be studied from a purely mathematical point of view. For example, many methods in computer vision are based on statistics, optimization or geometry. Finally, a significant part of the field is devoted to the implementation aspect of computer vision; how existing methods can be realized in various combinations of software and hardware, or how these methods can be modified in order to gain processing speed without losing too much performance.

Related fields

Computer vision, Image processing, Image analysis, Robot vision and Machine vision are closely related fields. If you look inside text books which have either of these names in the title there is a significant overlap in terms of what techniques and applications they cover. This implies that the basic techniques that are used and developed in these fields are more or less identical, something which can be interpreted as there is only one field with different names.

On the other hand, it appears to be necessary for research groups, scientific journals, conferences and companies to present or market themselves as belonging specifically to one of these fields and, hence, various characterizations which distinguish each of the fields from the others have been presented. The following characterizations appear relevant but should not be taken as universally accepted.

Image processing and Image analysis tend to focus on 2D images, how to transform one image to another, e.g., by pixel-wise operations such as contrast enhancement, local operations such as edge extraction or noise removal, or geometrical transformations such as rotating the image. This characterization implies that image processing/analysis does not produce nor require assumptions about what a specific image is an image of.

Computer vision tends to focus on the 3D scene projected onto one or several images, e.g., how to reconstruct structure or other information about the 3D scene from one or several images. Computer vision often relies on more or less complex assumptions about the scene depicted in an image.

Machine vision tends to focus on applications, mainly in industry, e.g., vision based autonomous robots and systems for vision based inspection or measurement. This implies that image sensor technologies and control theory often are integrated with the processing of image data to control a robot and that real-time processing is emphasized by means of efficient implementations in hardware and software.

There is also a field called Imaging which primarily focus on the process of producing images, but sometimes also deals with processing and analysis of images. For example, Medical imaging contains lots of work on the analysis of image data in medical applications.

Finally, pattern recognition is a field which uses various methods to extract information from signals in general, mainly based on statistical approaches. A significant part of this field is devoted to applying these methods to image data.

A consequence of this state of affairs is that you can be working in a lab related to one of these fields, apply methods from a second field to solve a problem in a third field and present the result at a conference related to a fourth field!

Examples of applications for computer vision

Another way to describe computer vision is in terms of applications areas. One of the most prominent application fields is medical computer vision or medical image processing. This area is characterized by the extraction of information from image data for the purpose of making a medical diagnosis of a patient. Typically image data is in the form of microscopy images, X-ray images, angiography images, ultrasonic images, and tomography images. An example of information which can be extracted from such image data is detection of tumours, arteriosclerosis or other malign changes. It can also be measurements of organ dimensions, blood flow, etc. This application area also supports medical research by providing new information, e.g., about the structure of the brain, or about the quality of medical treatments.

A second application area in computer vision is in industry. Here, information is extracted for the purpose of supporting a manufacturing process. One example is quality control where details or final products are being automatically inspected in order to find defects. Another example is measurement of position and orientation of details to be picked up by a robot arm. See the article on machine vision for more details on this area.

Military applications are probably one of the largest areas for computer vision, even though only a small part of this work is open to the public. The obvious examples are detection of enemy soldiers or vehicles and guidance of missiles to a designated target. More advanced systems for missile guidance send the missile to an area rather than a specific target, and target selection is made when the missile reaches the area based on locally acquired image data. Modern military concepts, such as "battlefield awareness," imply that various sensors, including image sensors, provide a rich set of information about a combat scene which can be used to support strategic decisions. In this case, automatic processing of the data is used to reduce complexity and to fuse information from multiple sensors to increase reliability.

One of the newer application areas is autonomous vehicles, which include submersibles, land-based vehicles (small robots with wheels, cars or trucks), and aerial vehicles. An unmanned aerial vehicle is often denoted UAV. The level of autonomy ranges from fully autonomous (unmanned) vehicles to vehicles where computer vision based systems support a driver or a pilot in various situations. Fully autonomous vehicles typically use computer vision for navigation, i.e. for knowing where it is, or for producing a map of its environment (SLAM) and for detecting obstacles. It can also be used for detecting certain task specific events, e. g., a UAV looking for forest fires. Examples of supporting system are obstacle warning systems in cars and systems for autonomous landing of aircraft. Several car manufacturers have demonstrated systems for autonomous driving of cars, but this technology has still not reached a level where it can be put on the market. There are ample examples of military autonomous vehicles ranging from advanced missiles to UAVs for recon missions or missile guidance. Space exploration is already being made with autonomous vehicles using computer vision, e. g., NASA's Mars Exploration Rover.

Other application areas include the creation of visual effects for cinema and broadcast, e.g., camera tracking or matchmoving, and surveillance.

Typical tasks of computer vision

Object recognition

Detecting the presence of known objects or living beings in an image, possibly together with estimating the pose of these objects.

Examples: Searching in digital images for specific content (content-based image retrieval) Recognizing human faces and their location in images. Estimation of the three-dimensional pose of humans and their limbs Detection of objects which are passing through a manufacturing process, e.g., on a conveyor belt, and estimation of their pose so that a robot arm can pick up the objects from the belt.

Optical character recognition

OCR (optical character recognition) takes pictures of printed or handwritten text and converts it into computer readable text such as ASCII or Unicode. In the past images were acquired with a computer scanner, however more recently some software can also read text from pictures taken with a digital camera.

Tracking

Tracking known objects through an image sequence.

Examples: Tracking a single person walking through a shopping center. Tracking of vehicles moving along a road.

Scene interpretation

Creating a model from an image/video.

Examples: Creating a model of the surrounding terrain from images, which are being taken by a robot-mounted camera. Anticipating the pattern of the image to determine size and density to estimate the volume using tomography like device. The cloud recognition is one the government project using this method.

Egomotion

The goal of egomotion computation is to describe the motion of an object with respect to an external reference system, by analyzing data acquired by sensors on-board on the object. i.e. the camera itself.

Examples: Given two images of a scene, determine the 3d rigid motion of the camera between the two views.

Computer vision systems

A typical computer vision system can be divided in the following subsystems:

Image acquisition

The image or image sequence is acquired with an imaging system (camera, radar, lidar, tomography system). Often the imaging system has to be calibrated before being used.

Preprocessing

In the preprocessing step, the image is being treated with "low-level"-operations. The aim of this step is to do noise reduction on the image (i.e. to dissociate the signal from the noise) and to reduce the overall amount of data. This is typically being done by employing different (digital)image processing methods such as: Down-sampling the image. Applying digital filters convolutions, computing a scale space representation Correlations or linear shift invariant filters Sobel operator Computing the x- and y-gradient (possibly also the time-gradient). Segmenting the image. Pixelwise thresholding. Performing an eigentransform on the image Fourier transform Doing motion estimation for local regions of the image (also known as optical flow estimation). Estimating disparity in stereo images. Multiresolution analysis

Feature extraction

The aim of feature extraction is to further reduce the data to a set of features, which ought to be invariant to disturbances such as lighting conditions, camera position, noise and distortion. Examples of feature extraction are: Performing edge detection or estimation of local orientation. Extracting corner features. Detecting blob features. Extracting spin images from depth maps. Extracting geons or other three-dimensional primitives, such as superquadrics. Acquiring contour lines and maybe curvature zero crossings. Generating features with the Scale-invariant feature transform.

Registration

The aim of the registration step is to establish correspondence between the features in the acquired set and the features of known objects in a model-database and/or the features of the preceding image. The registration step has to bring up a final hypothesis. To name a few methods: Least squares estimation Hough transform in many variations Geometric hashing Particle filtering RANdom SAmple Consensus.

Appendix C. Traffic sign recognition mobile mapping adquisition

The Traffic Sign Recognition (TSR) is a field of applied computer vision research concerned with the automatical detection and classification of traffic signs in traffic scene images acquired from a moving car. Most part of the work done in this field is enclosed in the problem of the Intelligent Transportation Systems (ITS), which aim is to provide Driver Support Systems (DSS) with the ability to understand its neighborhood environment and so permit advanced driver support such as collision prediction and avoidance. Driving is a task based fully on visual information processing. The road signs and traffic signals define a visual language interpreted by drivers. Road signs carry many information necessary for successful driving - they describe current traffic situation, define right-of-way, prohibit or permit certain directions, warn about risky factors, etc. Road signs also help drivers with navigation. Two basic applications of TSR are under consideration in the research community - driver's aid (DSS) and automated surveillance of road traffic devices. It is desirable to design smart car control systems in such a way to allow evolution of fully autonomous vehicles in the future. The TSR system is also being considered as the valuable complement of the GPS-based navigation system. The dynamical environmental map may be enriched by road sign types and positions (acquired by TSR) and so help with the precision of current vehicle position.

Mobile mapping: the Geomobil project on Mobile mapping is a useful technique used to compile cartographic information from a mobile vehicle. The mobile vehicle is usually equipped with a set of sensors synchronized with an orientation system in order to link the obtained information with its position over the map. We are working with the mobile mapping system named Geomobil. The Geomobil is a Land Based Mobile Mapping System (LBMMS) developed by the Institut Cartogràfic de Catalunya (ICC) (fig. 1). It is a modular system that allows the direct orientation of any sensor mounted on a roof platform. The Geomobil system is composed of the following subsystems: orientation subsystem, image subsystem, laser ranging subsystem, synchronization subsystem, power and environmental control subsystem. In our case we only use information from the image and orientation subsystems, which will be briefly explained in the rest of this point.

Geomobil system: the orientation subsystem is responsible for georeferencing the images acquired by the Geomobil. Thus it provides the coordinates (position) and the angles (attitude) of their projection centers. It is a system that combines inertial and GPS observations at a high level of integration, where the GPS derived trajectories are used to correct and calibrate the drifts of the Inertial Measurement Unit (IMU) gyros and accelerometers so that the position and velocity errors derived from inertial sensors are minimized. This combination of GPS and IMU systems allows the system to calculate the position even when the GPS satellites signals are blocked by terrain conditions (buildings, bridges, tunnels,...). The image subsystem design has been driven by two main requirements: to acquire images of at least 1Mpix and to get 10m stereoscopic overlap at a 10m distance from the van.

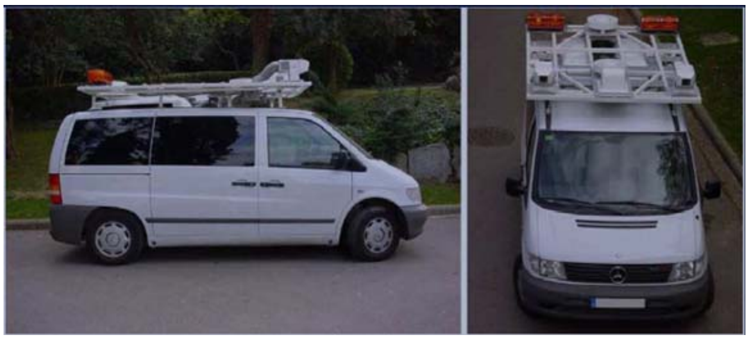

Fig. 1. Geomobil system.

The stereo overlap is conditioned by two factors: getting the maximum stereoscopic overlap free of obstacles and preserving a B/D ratio (stereoscopic Base - object Distance) as good as possible.

The system links the captured images with their position and orientation data, and saves the information to the discs. The acquisition frequency is limited by the storage system capacity, and nowadays is programmed to take a stereo-pair of images each 10 meters or a turn higher than 60 degrees, which corresponds to the camera field of view.

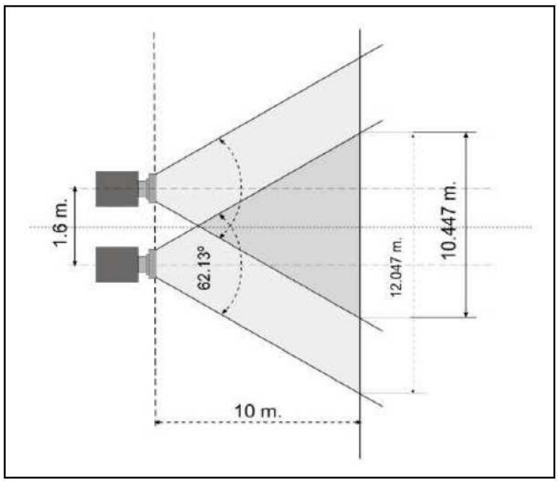

Fig. 2. Stereoscopic system diagram. We can see the relation between overlap zone and distance. The Geovan has a pair of grey-scale cameras of 1024 × 1020, which parameters are shown in fig. 3.

Feature	Value
Number of pixels	1024×1020
Pixel size	$12\mu m$
Focal length	$10.2mm$
FOV	62.13^o
IFOV	3 min. 38 sec.
Precision at $10m$ (across-track)	$0.8cm$
Precision at $10m$ (along-track)	$5.6cm$

Fig. 3. Geovan camera characteristics.

Appendix D. Sony Aibo specifications

Aibo specifications 1:

1 Stereo microphones Allow the AIBO Entertainment Robot to listen to the surrounding environment.
2 Head distance sensor Measures the distance between the AIBO robot and other objects.
3 Color camera Detects the color, shape, and movement of nearby objects.
4 Mouth Picks up the AIBO toy and expresses emotions.
5 Chest distance sensor Measures the distance between the AIBO robot and other objects.
6 Tail Moves up, down, left, and right to express the AIBO robots emotions.
7 Ears Indicates the AIBO robots emotions and condition.
8 Head sensor Detects and turns white when you gently stroke the AIBO robot head.
9 Wireless light (on the back of the AIBO robots head) Indicator used with the wireless LAN function. This light turns blue when the AIBO robot is connected to the e-mail server.
10 Pause button When pressed, the AIBO robots activity will pause or resume.
11 Back sensors (front, middle, and rear) Detect and turn white when you gently stroke the AIBO robots back.
12 Face lights (illuminated face) These lights turn various colors to show the AIBO robots emotions and conditions.
13 **Head light** Detects and turns white when you touch the head sensor. Lights / flashes orange when one of the AIBO robots joints is jammed.
14 Mode indicators (inner side of ears) To indicate the present mode and condition of the AIBO robot.
15 Operation light During operation: turns green. During preparation for shutdown: it flashes green. During charging: it turns orange. When a charging error occurs: it flashes orange. When operation stops: it turns OFF. Outside hours of activity (Sleeping on the Energy Station): it slowly flashing green.
16 Back lights (front, middle, and rear) Detect and turn white when you gently touch the AIBO robots back sensors. These lights also turn blue (front), orange (middle), and red (rear) to indicate a variety of actions.

Sony Aibo specifications 2:

1 Paw sensors These are located on the bottom of the AIBO Entertainment Robot.s paws, and detect contact with any surface it touches. When the AIBO robot extends one of its paws, it will react with happiness if you touch it.
2 Speaker Emits music, sound effects, and voice guide.
3 Charging terminal When you place the AIBO robot on the Energy Station, this

part makes contact with the station to allow charging of the AIBO robots battery.
4 Volume control switch (VOLUME) Adjusts the volume of the speaker to one of four levels (including no sound).
5 Wireless LAN switch (WIRELESS) This turns the AIBO robots wireless LAN function ON or OFF.
6 Memory Stick media access indicator This indicator turns red while the AIBO robot is reading or writing to a Memory Stick media. While the indicator is ON, you cannot remove the Memory Stick media or battery by means of the Memory Stick media eject button (Z) or the battery latch (Z). Under this circumstance, never attempt to forcibly remove the Memory Stick media.
7 Battery pack latch (BATT Z) Flip this latch to the rear when you want to remove the battery.
8 Chin sensor Senses when you touch the AIBO robots chin.
9 FCC ID/MAC address label Indicates the FCC ID and MAC address of the AIBO robots wireless unit.
10 Battery slot Holds the AIBO robots lithium-ion battery
11 Memory Stick media eject button (Z) Press to eject the Memory Stick media.
12 Memory Stick media slot This is where you insert the provided AIBO-ware Memory Stick media.
*** Emergency eject hole** If you experience difficulties ejecting the Memory Stick media or battery because of a malfunction or operation problems, place the AIBO robot in Pause mode, and then insert an object such as a paper clip into the emergency eject hole. (Do not use fragile objects, such as toothpicks, into the emergency eject hole as they may break.) Under normal circumstances, you do not need to use the emergency eject hole.

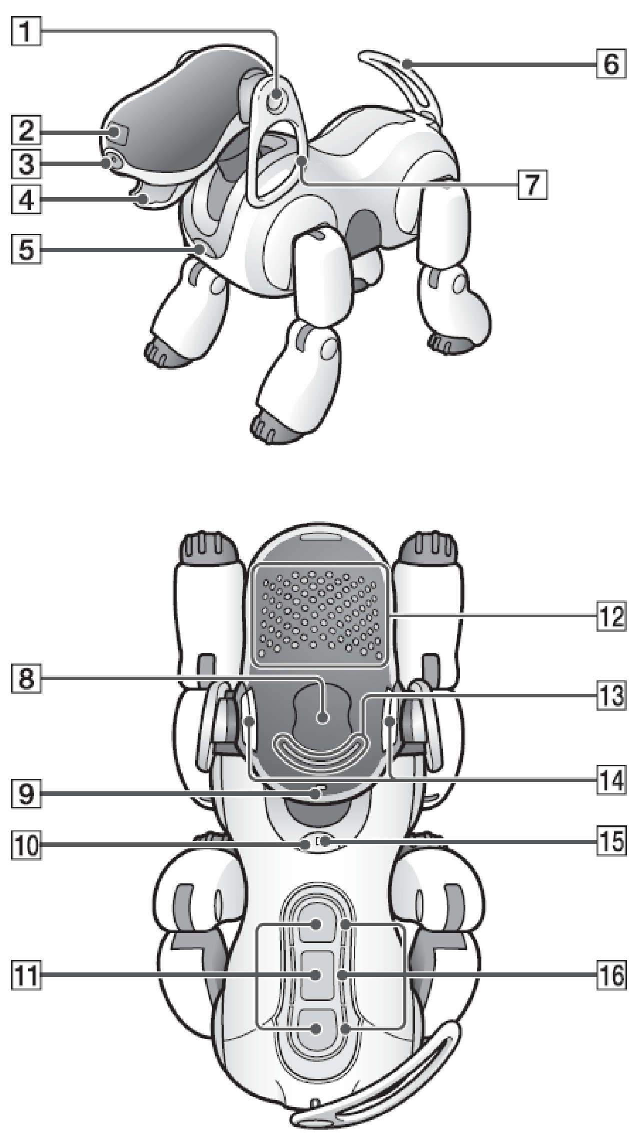

Fig. 4 Aibo specifications 1.

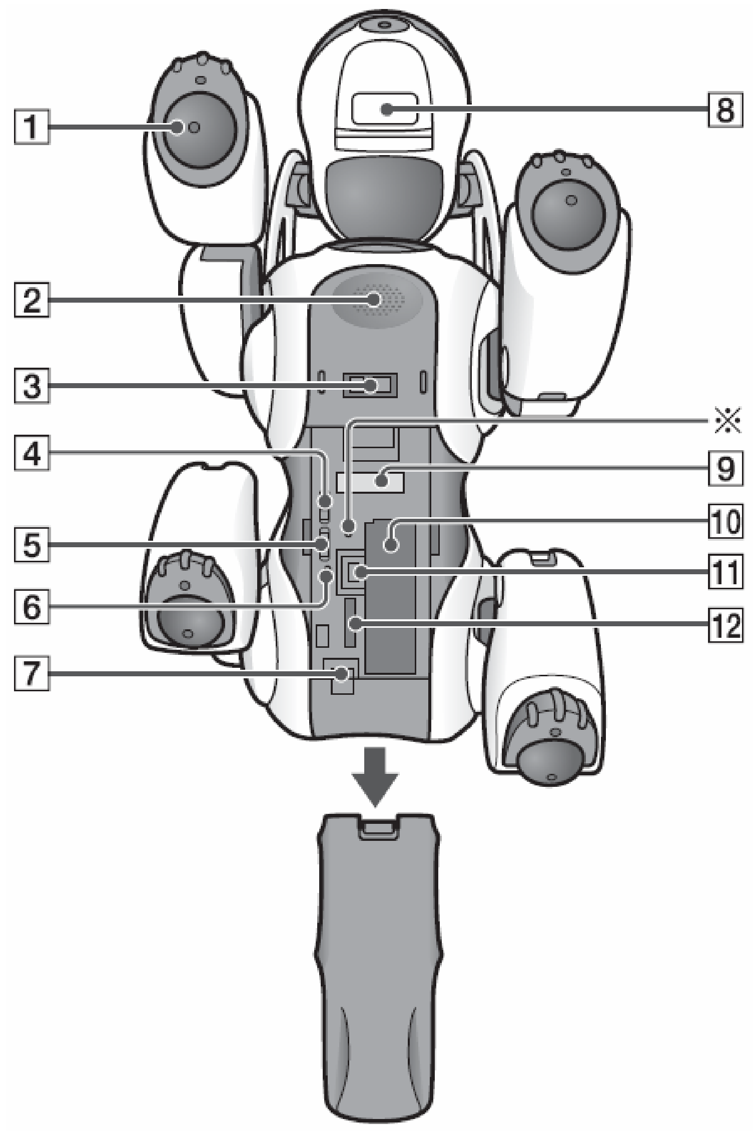

Fig. 5 Aibo specifications 2.

Appendix E. Application source code: main structures and functions.

```
typedef struct
{
        int cl;
        int acc;
} Flda;
Flda *flda;
static int cmpf( const void* _a, const void* _b)
{
   double a = *(double*)_a;
   double b = *(double*)_b;

        if(a < b) return -1;
  else if(a > b) return 1;
  else {return 0;}
}
int ncl;
int maxacccl(Flda *flda)
{
        Flda t;
        int i;
        t.cl=flda[0].cl;
        t.acc=flda[0].acc;
        for (i=1;i<ncl;i++)
        {
                if (flda[i].acc>t.acc)
                {
                        t.cl=flda[i].cl;
                        t.acc=flda[i].acc;
                }
        }
        return(t.cl);

}
int calccl(Flda* flda,int cl)
{
        int i;
        i=0;
        while (flda[i].cl!=cl && i<ncl)
        {
                i++;
        }
        return i;
}
typedef struct
{
        int cl1;
        int cl2;

        CvMat *mat;
        int nA;
        int nB;
        int * nsA;
        int * nsB;
}Fldadata;
Fldadata *fldadata;
int nflda;
void IniFlda(long int imgsize)
{
        char *filelist="filelist.txt";
        FILE *fl,*f;
        double value,nA,nB;
        int ncl;
        int n;
        int i,tmp,j;
        int c1,c2;
        char fname[255];
        fl=fopen(filelist,"r");
        fscanf(fl,"%d",&ncl);
        flda=malloc(ncl*sizeof(Flda));
        nflda=0;
        for (i=0;i<ncl;i++)
                nflda+=i;
        for (i=0;i<ncl;i++)
        {
                fscanf(fl,"%d",&tmp);
                flda[i].cl=tmp;
                flda[i].acc=0;
        }
        fldadata=malloc(nflda*sizeof(Fldadata));
   for (i=0;i<nflda;i++)
        {
                fscanf(fl,"%d %d %s",&c1,&c2,fname);


                fldadata[i].cl1=c1;
                fldadata[i].cl2=c2;
                fldadata[i].mat=cvCreateMat(1,imgsize,CV_64FC1);
                f=fopen(fname,"r");
                fscanf(f,"%lf",&value);
                fscanf(f,"%lf",&value);

                for (j=0;j<imgsize;j++)
                {
                        fscanf(f,"%lf",&value);
                        cvSetAt(fldadata[i].mat,cvScalar(value,0,0,0),0,j);
                }
                fscanf(f,"%lf",&nA);
                fscanf(f,"%lf",&nB);
                fldadata[i].nA=nA;
                fldadata[i].nB=nB;
                fldadata[i].nsA=malloc(fldadata[i].nA*sizeof(int));
                fldadata[i].nsB=malloc(fldadata[i].nB*sizeof(int));

                for (j=0;j<fldadata[i].nA;j++)
                {
                        fscanf(f,"%lf",&value);
                        fldadata[i].nsA[j]=value;
                }
                for (j=0;j<fldadata[i].nB;j++)
                {
                        fscanf(f,"%lf",&value);
                        fldadata[i].nsB[j]=value;
                }
                fclose(f);
        }
fclose(fl);

}
int clasflda(IplImage *img,int kn)
{
        char *filelist="filelist.txt";
        FILE *fl,*f;
        int i,tmp,j;
        int c1,c2,ce1,ce2;
        double nA,nB;
        char  fname[100];
        char lastname[100];
        double value,sum,e1,e2;
        int t1,t2;
        CvMat *mat,*imgmat,*rimgmat,*rtimgmat;
   CvMemStorage* storagetempA;
   CvMemStorage* storagetempB;
   CvSeq* seqA;
   CvSeq* seqB;
                storagetempA = cvCreateMemStorage(0);
                storagetempB = cvCreateMemStorage(0);
                seqA = cvCreateSeq( CV_64FC1, /* sequence of integer elements */
                                                  sizeof(CvSeq), /* header size - no extra
fields */
                  sizeof(double), /* element size */
                  storagetempA /* the container storage */ );
                seqB = cvCreateSeq( CV_64FC1, /* sequence of integer elements */
                  sizeof(CvSeq), /* header size - no extra fields */
                  sizeof(double), /* element size */
                  storagetempB /* the container storage */ );
        imgmat=cvCreateMatHeader(img->height,img->width,CV_8UC1);
imgmat=cvGetMat(img,imgmat,NULL,0);
        rtimgmat=cvCreateMat(img->height,img->width,CV_64FC1);
        rimgmat=cvCreateMat(img->height*img->width,1,CV_64FC1);
        cvConvertScale(imgmat,rtimgmat,1,0);
        cvReshape(rtimgmat,rimgmat,1,1);

        for (j=0;j<nflda;j++)
        {

                sum=cvDotProduct(fldadata[j].mat,rimgmat);
                sum=sum/255.0;
                for (i=0;i<fldadata[j].nA;i++)
                {
                        value=fldadata[j].nsA[i];
                        value=value-sum;
                        value*=(value<0? -1:1);
                        cvSeqPush(seqA,&value);
                }
                cvSeqSort(seqA,cmpf,0);
                for (i=0;i<fldadata[j].nB;i++)
                {
                        value=fldadata[j].nsB[i];
                        value=value-sum;
                        value*=(value<0? -1:1);
                        cvSeqPush(seqB,&value);
                }
                cvSeqSort(seqB,cmpf,0);
                e1=*(double*)cvGetSeqElem( seqA, 0 );
                e2=*(double*)cvGetSeqElem( seqB, 0 );
                i=0;
                ce1=0;
                ce2=0;

                c1=calccl(flda,fldadata[j].cl1);
                c2=calccl(flda,fldadata[j].cl2);
                while (i<kn)
                {
                        if (e1<e2)
                        {
                                ce1++;
                                e1=*(double*)cvGetSeqElem(seqA,ce1);
                        } else
                        {
                                ce2++;
                                e2=*(double*)cvGetSeqElem(seqB,ce2);
                        }
                        i++;
                }
                if (ce1>ce2)
```

```
                        {
                                flda[c1].acc++;
                        } else
                        {
                                flda[c2].acc++;
                        }
                        cvClearSeq(seqA);
                        cvClearSeq(seqB);

                }

return maxacccl(flda);
}


int valid=1;

IplImage *detecta2(IplImage *imgO);


typedef struct Class
{
   float dif;
   int y;
}
Class;

typedef struct structClass
{
   CvRect* rectangulo;
   int clase_final;
}
structClass;

static int cmp_func( const void* _a, const void* _b)
{
   float* a = (float*)_a;
   float* b = (float*)_b;

        if(a[4] < b[4]) return 1;
  else if(a[4] > b[4]) return -1;
  else {if(a[5] < b[5]) return 1;
                else if(a[5] > b[5]) return -1;
                        else return 0;}
}

static int cmp_func2( const void* _a, const void* _b)
{
   Class* a = (Class*)_a;
   Class* b = (Class*)_b;
```

```
            if(a->dif < b->dif) return -1;
   else if(a->dif > b->dif) return 1;
   else {return 0;}
}

float angulo( int a, int b)
{

            float aux;
            float F;

            if(a==0){
                        if(b>0){
                                    F=(float)(CV_PI/2);
                        }else{ F=(float)((3*CV_PI)/2);}
            }else{
                        if (b==0){
                                    if(a>0) F=0;
                                    else F=(float)CV_PI;
                                    }

                        else{
                                                aux= (float)atan2(b,a);
                                                if(a>0 && b>0) F=(float)(CV_PI-aux);
                                                if(a<0 && b<0) F=-aux;
                                                if(a>0 && b<0) F=-aux;
                                                if(a<0 && b>0) F=(float)(aux+CV_PI);
                                    }
                        }
            F=(float)((F*360)/(2*CV_PI));
            return F;



}
CvPoint interseccion( CvPoint a1 ,  CvPoint a2 , CvPoint b1 , CvPoint b2)
{
    CvPoint tall;
            int x_tall;
            int y_tall;

            float m1=(float) (a2.y - a1.y)/(a2.x - a1.x);
            float m2=(float) (b2.y - b1.y)/(b2.x - b1.x);

            float c1= a1.y - (m1 * a1.x);
            float c2= b1.y - (m2 * b1.x);

            x_tall=(int)((c2-c1)/(m1-m2));
            y_tall=(int)(m1*x_tall+c1);
```

```
        tall = cvPoint(x_tall,y_tall);

        return tall;


}

IplImage* drawSquares( IplImage* imagen, CvSeq* clases )
{
        CvFont fuente;
        CvPoint pt1,pt2;
        CvRect* r;
        char texto[2];
        structClass* numero;
   int i;
        //Inicializamos la fuente
        cvInitFont(&fuente, CV_FONT_VECTOR0,0.8,0.8,0,2,8);

   // Leemos 4 elementos de la secuencia al mismo tiempo(vertices del rectangulo)
   for( i = 0; i < clases->total; i ++ )
   {

      numero = ( structClass* )cvGetSeqElem( clases , i);
                r= numero->rectangulo;
                pt1.x = r->x;
                pt2.x = r->x + r->width;
                pt1.y = r->y;
                pt2.y = r->y + r->height;

      // Pintamos el rectangulo
                cvRectangle( imagen, pt1, pt2, CV_RGB(255,0,0), 3, 8, 0);

                // Pintamos el texto
                printf("%d\n",numero->clase_final);
                itoa(numero->clase_final,texto,10);

                cvPutText( imagen, texto, cvPoint(pt2.x - (r->width/2),pt2.y + 25),
&fuente, CV_RGB(255,255,0));

   }

        return imagen;

}


IplImage* transform( IplImage* origen, IplImage* destino,IplImage*  mascara ,CvPoint
int1 ,  CvPoint int2 , CvPoint int3 )
{
```

```
                CvPoint2D32f sp[4];
                CvPoint2D32f dp[4];

                double m[9];
                CvMat map_matrix = cvMat( 3, 3, CV_64F, m );


                sp[0] = cvPoint2D32f(int1.x,int1.y);
                sp[1] = cvPoint2D32f(int2.x,int2.y);
                sp[2] = cvPoint2D32f(int3.x,int3.y);
                sp[3] = cvPoint2D32f((int1.x+int2.x+int3.x)/3,(int1.y+int2.y+int3.y)/3);

                dp[0] = cvPoint2D32f(21,0);
                dp[1] = cvPoint2D32f(0,38);
                dp[2] = cvPoint2D32f(43,38);
                dp[3] = cvPoint2D32f(64/3,76/3);

                cvWarpPerspectiveQMatrix( sp, dp, &map_matrix );
                m[8] = 1.; // workaround for the bug

                cvWarpPerspective( origen,destino , &map_matrix,
CV_INTER_LINEAR+CV_WARP_FILL_OUTLIERS,cvScalarAll(0));
                cvEqualizeHist(destino , destino);

                cvAnd( destino, mascara, destino, 0 );

                return destino;

}


int clasif( IplImage* origen, char nombre[] ,int* clases[] ,int width ,int height  )
{
                int conta=0;
                int i;
                IplImage* a = cvCreateImage( cvSize(width,height), 8, 1 );
                IplImage* b = cvCreateImage( cvSize(width,height), 8, 1 );
                IplImage* clase;
                CvScalar resto;
                Class diff;
                Class* diff2;
                int clasres[10];
                char num[2];
                char nombref[100];
                CvMat* pnt3=0;
                CvMemStorage* storagetemp = cvCreateMemStorage(0);
                CvSeq* seq = cvCreateSeq( CV_32FC2, /* sequence of integer elements
*/
                  sizeof(CvSeq), /* header size - no extra fields */
```

```
        sizeof(Class), /* element size */
        storagetemp /* the container storage */ );

      pnt3 = cvCreateMat( origen->width, origen->height, CV_32FC1 );


      for(conta=0; conta< 22 ; conta++)
      {

            sprintf(nombref,"%s%d_knn.jpg",nombre,clases[conta]);

            if( (clase = cvLoadImage(nombref, 0))!= 0)
            {

                  for(i=0; i<(clase->height); i++)
                  {
                        pnt3 = cvGetRow( clase, pnt3, i);

                        cvReshape( pnt3, pnt3, 0, height);
                        cvGetImage (pnt3, a);


                        cvAbsDiff( origen, a, b);



                        cvPow( b, b, 2 );
                        resto = cvSum( b );


                        diff.dif=(float)sqrt((float)resto.val[0]);
                                                diff.y=clases[conta];

                        cvSeqPush( seq, &diff );
                  }

            }else{printf("El fichero de clase no existe\n");}
      }
      cvSeqSort( seq, cmp_func2, 0 );
      for( i = 0; i < 3; i++ )
      {


            diff2 = (Class*)cvGetSeqElem( seq, i );
            clasres[i]=diff2->y;
}
      if(clasres[0]==clasres[1] || clasres[0]==clasres[2])
      {

            return clasres[0];
```

```
                }else{
                                if(clasres[1]==clasres[2]){

                                        return clasres[1];

                                }else{
                                                return clasres[0];

                                                }


                        }


                        cvReleaseImage( &a );
                        cvReleaseImage( &b );
                        cvReleaseImage( &clase );
                        cvReleaseMemStorage(&storagetemp);
   }



IplImage* detecta(IplImage* src2)
{
      IplImage* src = cvCreateImage( cvGetSize(src2), 8, 1 );
                IplImage* dst = cvCreateImage( cvGetSize(src2), 8, 1 );
      IplImage* color_dst = cvCreateImage( cvGetSize(src2), 8, 3 );
                IplImage* color_dst2 = cvCreateImage( cvSize(44,39), 8, 3 );
                IplImage* color_dst3 = cvCreateImage( cvSize(44,39), 8, 1 );

                IplImage* mask = cvLoadImage("mask.jpg", 0);

                float*  p1;
                int N= 6;
                int S;
                int contador=0;
                int recta1=0;
                int recta2=0;
                int recta3=0;

                char finnom[]=".jpg";

                int num[3]={0,1,2};


                CvPoint interseccion1,interseccion2,interseccion3;
                CvMat* dist=0;
                CvMat* pnt3=0;
                double m[9];
                CvMat map_matrix = cvMat( 3, 3, CV_64F, m );*/


                CvPoint punto11,punto12, punto21,punto22,punto31,punto32;
        CvMemStorage* storage = cvCreateMemStorage(0);
        CvSeq* lines = 0;

                CvMemStorage* storagetemp = cvCreateMemStorage(0);
                CvSeq* seq = cvCreateSeq( CV_32FC2, /* sequence of integer elements
*/
                  sizeof(CvSeq), /* header size - no extra fields */
                  sizeof(Class), /* element size */
                  storagetemp /* the container storage */ );

        int i;


            cvCvtColor( src2, src, CV_BGR2GRAY);


        cvCanny( src, dst, 48, 80, 3 );


                cvCvtColor( dst, color_dst, CV_GRAY2BGR );
                      lines = cvHoughLines2( dst, storage,
CV_HOUGH_PROBABILISTIC, 1, CV_PI/180, 9, 5, 2);
                dist = cvCreateMat( lines->total, 6, CV_32FC1 );

        for( i = 0; i < lines->total; i++ )
        {

                        CvPoint* line = (CvPoint*)cvGetSeqElem(lines,i);
                        CV_MAT_ELEM(*dist, int, i, 0)=line[0].x;
                        CV_MAT_ELEM(*dist, int, i, 1)=line[0].y;
                        CV_MAT_ELEM(*dist, int, i, 2)=line[1].x;
                        CV_MAT_ELEM(*dist, int, i, 3)=line[1].y;
                        CV_MAT_ELEM(*dist, float, i, 4)=(float)sqrt(pow((line[1].x-
line[0].x),2) + pow((line[1].y-line[0].y),2));
          CV_MAT_ELEM(*dist, float, i, 5)=angulo((line[0].x-line[1].x),(line[0].y-
line[1].y));



                }


                (float *)p1 = dist->data.fl;
                S= dist->step;
                qsort(p1,lines->total,S, cmp_func);

                i=0;

                while(contador<=3 && i<(lines->total))
                 {


                        if(dist->data.fl[i*6+5]>45 && dist->data.fl[i*6+5]<75 &&
recta1==0){

                                recta1=1;


                                punto11= cvPoint(CV_MAT_ELEM(*dist, int, i, 0),
CV_MAT_ELEM(*dist, int, i, 1));
                                punto12= cvPoint(CV_MAT_ELEM(*dist, int, i, 2),
CV_MAT_ELEM(*dist, int, i, 3));
        contador++;}
                        if(dist->data.fl[i*6+5]>105 && dist->data.fl[i*6+5]<135 &&
recta2==0){


                                punto21= cvPoint(CV_MAT_ELEM(*dist, int, i, 0),
CV_MAT_ELEM(*dist, int, i, 1));
                                punto22= cvPoint(CV_MAT_ELEM(*dist, int, i, 2),
CV_MAT_ELEM(*dist, int, i, 3));

                                recta2=1;
        contador++;}
                         if(dist->data.fl[i*6+5]>-15 && dist->data.fl[i*6+5]<15 &&
recta3==0){


                                punto31= cvPoint(CV_MAT_ELEM(*dist, int, i, 0),
CV_MAT_ELEM(*dist, int, i, 1));
                                punto32= cvPoint(CV_MAT_ELEM(*dist, int, i, 2),
CV_MAT_ELEM(*dist, int, i, 3));
                                recta3=1;
                        contador++;}
                         if(dist->data.fl[i*6+5]>165 && dist->data.fl[i*6+5]<195 &&
recta3==0){


                                punto31= cvPoint(CV_MAT_ELEM(*dist, int, i, 0),
CV_MAT_ELEM(*dist, int, i, 1));
                                punto32= cvPoint(CV_MAT_ELEM(*dist, int, i, 2),
CV_MAT_ELEM(*dist, int, i, 3));
                                recta3=1;
                                contador++;}
                         if(contador==3 && (punto31.y < punto11.y && punto31.y <
punto12.y) && (punto31.y < punto21.y && punto31.y < punto22.y)){
                                contador--;
                                recta3=0;}
                         i++;
                 }

                 interseccion1 =interseccion(punto11,punto12,punto21,punto22);
                 interseccion2 =interseccion(punto11,punto12,punto31,punto32);
                 interseccion3 =interseccion(punto31,punto32,punto21,punto22);

                 valid=1;

                 if((interseccion1.x==0 && interseccion1.y==0) || (interseccion2.x==0
&& interseccion2.y==0) || (interseccion3.x==0 && interseccion3.y==0))
                 {
                         valid=0;
                        printf("una de las rectas no es valida");
                 }

                color_dst3= transform( src , color_dst3 , mask , interseccion1 ,
interseccion2 , interseccion3 );


                cvReleaseMat(&pnt3);
                cvReleaseMat(&dist);
                cvReleaseImage( &src );
                cvReleaseImage( &dst );
                cvReleaseImage( &color_dst );
                cvReleaseImage( &color_dst2 );
                cvReleaseMemStorage(&storage);
                cvReleaseMemStorage(&storagetemp);
                return (color_dst3);



}


CvSeq* detect_and_draw( IplImage* img ,char cascada[])
{
   int scale = 1;
   IplImage* temp = cvCreateImage( cvSize(img->width/scale,img->height/scale), 8, 3
);
   CvPoint pt1, pt2;
   int i;
        int clase;
        int num[3];
        CvHaarClassifierCascade* cascade;
        IplImage* R;
        IplImage* C;
        IplImage* Captura;
        CvRect* r;
        CvMemStorage* storage2= cvCreateMemStorage(0);
        CvMemStorage* storagetemp2 = cvCreateMemStorage(0);
        char tipo;

        CvSeq* secuencia =
cvCreateSeq(CV_32FC2,sizeof(CvSeq),sizeof(structClass),storagetemp2);
        structClass resultado;

   cvClearMemStorage( storage2 );
        cascade = (CvHaarClassifierCascade*)cvLoad( cascada, 0, 0, 0 );

        if (strcmp(cascada,"cascada_circular.xml"))
        {
                tipo=0;
                num[0]=0;
                num[1]=1;
                num[2]=2;
        } else
        {
                tipo=1;
                num[0]=3;
                num[1]=4;
                num[2]=5;
        }

   if( cascade )
   {
      CvSeq* faces = cvHaarDetectObjects( img, cascade, storage2,
                                 1.1, 2, CV_HAAR_DO_CANNY_PRUNING,
                                 cvSize(40, 40) );

      for( i = 0; i < (faces ? faces->total : 0); i++ )
      {

                        r = (CvRect*)cvGetSeqElem( faces, i );

        pt1.x = r->x*scale;
        pt2.x = (r->x+r->width)*scale;
        pt1.y = r->y*scale;
        pt2.y = (r->y+r->height)*scale;

                        //Clonar imagen a recortar
                        C = cvCloneImage(img);
```

```
//Guardar la imagen recortada


cvSetImageROI(C,cvRect(pt1.x,pt1.y,r->width,r->height));
R = cvCreateImage( cvSize(r->width,r->height),8,3);
cvResize(C,R,CV_INTER_LINEAR);



//Paso por parametros a funcion
if (!tipo)
        Captura = detecta(R);
else
        Captura = detecta2(R);
if(valid==1){
        if (!tipo)
                clase = clasif(Captura,"./clases/clase",num ,44,39);
        else
                clase = clasif(Captura,"./clases/clase",num ,30,30);
        resultado.rectangulo = r;
        resultado.clase_final = clase;

        cvSeqPush(secuencia,&resultado);

        switch(resultado.clase_final)
        {
        case 0:
                printf("\nLa imagen es de la clase PELIGRO
FUEGO\n");
                break;
        case 1:
                printf("\nLa imagen es de la clase PELIGRO
GATO\n");
                break;
        case 2:
                printf("\nLa imagen es de la clase PELIGRO
TUNEL\n");
                break;
        case 3:
                printf("\nLa imagen es de la clase PELOTA\n");
                break;
        case 4:
                printf("\nLa imagen es de la clase HUESO\n");
                break;
        case 5:
                printf("\nLa imagen es de la clase CARA
SONRIENTE\n");
                break;
        default:
```

```
                                        printf("\nNO he podido clasificarla\n");

                                }




                        }
                                cvResetImageROI(C);

                }


                cvReleaseImage( &temp);
                cvReleaseHaarClassifierCascade(&cascade);
                return secuencia;

   }


}




IplImage *modulo,*canny,*acc;
CvMat *imgsxmat,*imgsymat,*modulmat,*imgsx2mat,*imgsy2mat,*scalemat;
CvMat *finalmat,*finalmat,*scaledmat1,*finalscaledmat;
double *modul;
int size;
float thres;

int calcacc(int rmin,int rmax, long int *a,char setzero,int *x,int *y,int *min,int *max)
{
        int radio=0;
        int cmax=0;
        int i,j,k;
        float px;
        float py;
        long int p;
        double c;
        int b1,b2;
        int x1,y1;
        for (i=0;i<size;i++)
                a[i]=0;
  for (k=rmin;k<rmax;k++)
  {
         if (setzero)
                for (i=0;i<size;i++)
                        a[i]=0;
```

```
    for (i=0;i<modulo->width;i++)
            {
                    for (j=0;j<modulo->height;j++)
                    {
                            if (modul[i+j*modulo->width]>thres)
                            {
                                    c=modul[i+j*modulo->width];
                                    b1=cvGetAt(imgsxmat,j,i).val[0];
                                    b2=cvGetAt(imgsymat,j,i).val[0];
                                    if (c)
                                    {
                                            px=k*b1;
                                            px=px/c;
                                            py=k*b2;
                                            py=py/c;
                                            p=px+i+(j+py)*modulo->width;
                                            if ((p < size) && (p>=0))
                                                    a[p]++;
                                            p=i-px+(j-py)*modulo->width;
                                            if ( p>= 0 && p<size)
                                                    a[p]++;
                              }

                            }
                    }

            }

            if (setzero)
            if (a[(*x)+(*y)*modulo->width]>cmax && k>rmin)
            {
                    radio=k;
                    cmax=a[(*x)+(*y)*modulo->width];
            }
}

if (!setzero)
{

        (*min)=2100000;
        (*max)=0;
        (*x)=0;
        (*y)=0;
        for (i=0;i<size;i++)
        {

                y1=i/acc->width;
```

```
                    x1=i%acc->width;

                    if (a[i]>(*max) && y1 < (0.6*acc->height) && x1<(0.6*acc->width)
&& y1>(0.4*acc->height) && x1>(0.4*acc->width))
                    {
                              *x=x1;
                              *y=y1;
                              *max=a[i];
                    }

    min=(a[i]<min? a[i]:min);
  }
}

return(radio);
}



IplImage *detecta2(IplImage *imgO,int height,int width)
{
  float mmax=0;
  int rmin;
  int rmax;
  unsigned char *rawdata;
  unsigned char *modulos;
    long int *a;
  int x,y,i,j;
  int min,max,radio;
          double scal;
          double macci=0;
          double maccj=0;
  IplImage* img         ;
  IplImage* imgs  ;
  IplImage* imgsx16;
  IplImage* imgsy16 ;
  IplImage* imgsx;
  IplImage* imgsy;

  IplImage* mask;
  CvPoint2D32f sp[4];
          CvPoint2D32f dp[4];

          double m[9];
          CvMat map_matrix;
  IplImage *finalimg,*finalscaledimg;
          unsigned char *final;
          unsigned char *finalscaled;
```

```
img     = cvCreateImage(cvGetSize(imgO),IPL_DEPTH_8U,1);
imgsx = cvCreateImage(cvGetSize(img),IPL_DEPTH_8U,1);
  imgsy = cvCreateImage(cvGetSize(img),IPL_DEPTH_8U,1);

imgs  = cvCloneImage(img);
imgsx16 = cvCreateImage(cvGetSize(img),IPL_DEPTH_16S,1);
imgsy16 = cvCreateImage(cvGetSize(img),IPL_DEPTH_16S,1);

  acc = cvCreateImage(cvGetSize(img),IPL_DEPTH_8U,1);
  modulo= cvCreateImage(cvGetSize(img),IPL_DEPTH_8U,1);
  canny = cvCreateImage(cvGetSize(img),IPL_DEPTH_8U,1);
  img=imgO;


  //El Gaussian y las derivadas
  cvSmooth( img, imgs, CV_GAUSSIAN,3,0,0);
  cvSobel( imgs, imgsx16, 1, 0,3);
  cvSobel( imgs, imgsy16, 0, 1,3);
  cvConvert(imgsx16,imgsx);
  cvConvert(imgsy16,imgsy);

  imgsxmat=cvCreateMatHeader(imgsx16->height,imgsx16->width,CV_16SC1);
  imgsymat=cvCreateMatHeader(imgsy16->height,imgsy16->width,CV_16SC1);

  imgsxmat=cvGetMat(imgsx16,imgsxmat,NULL,0);
  imgsymat=cvGetMat(imgsy16,imgsymat,NULL,0);

  size=imgsx16->height*imgsx16->width;


  rawdata=(unsigned char *) malloc(size);
  modulos=(unsigned char *)malloc(size);
  modul=(double *) malloc(size*sizeof(double));

  for (i=0;i<imgsx16->width;i++)
          for (j=0;j<imgsx16->height;j++)
     {
           double
tmp=cvGetAt(imgsxmat,j,i).val[0]*cvGetAt(imgsxmat,j,i).val[0]+cvGetAt(imgsymat,j,i
).val[0]*cvGetAt(imgsymat,j,i).val[0];
                  modul[i+j*imgsx16->width]=sqrt(tmp);
                  modulos[i+j*imgsx16->width]=(unsigned char)modul[i+j*imgsx16-
>width];
          }

 imgsx2mat=cvCreateMat(imgsx16->height,imgsx16->width,CV_16SC1);
 cvSetZero(imgsx2mat);
  cvMul (imgsxmat, imgsxmat, imgsx2mat,1);
```

```
imgsy2mat=cvCreateMat(imgsx16->height,imgsx16->width,CV_16SC1);
cvSetZero(imgsy2mat);
cvMul (imgsymat, imgsymat, imgsy2mat,1);



modulmat=cvCreateMat(imgsx16->height,imgsx16->width,CV_16SC1);
cvSetZero(modulmat);
cvAdd (imgsx2mat, imgsy2mat, modulmat,0);

 cvGetImage(modulmat,modulo);

  mmax=0;
  for (i=0;i<modulo->width;i++)
          for (j=0;j<modulo->height;j++)
                  mmax=(modulo->imageData[i+j*modulo->width]>mmax? modulo-
>imageData[i+j*modulo->width]:mmax);

  fflush(stdout);
  thres=0.1*mmax;
  cvCanny(imgs,canny,1,40,3);




  a=(long int *)malloc(size*sizeof(long int));

  rmin=img->width/5;
  rmax=img->width/2;

  //Calc acc mira entre rmin y rmax los vectores y acumula en a, scando el minimo y el
maximo, y la posicion del maximo
  calcacc(rmin,rmax,a,0,&x,&y,&min,&max);

  radio=calcacc(rmin,rmax,a,1,&x,&y,&min,&max);

  rmin=0.8*radio;
  rmax=1.3*radio;

  calcacc(rmin,rmax,a,0,&x,&y,&min,&max);

  radio=calcacc(rmin,rmax,a,1,&x,&y,&min,&max);


  //sanity check
  if (radio*2+1>=(img->width))
  {
          radio=img->width/2-1;
  }
```

```
for (i=0;i<size;i++)
{
        a[i]=255*(a[i]-min);
        rawdata[i]=a[i]/(max-min);
}
cvSetImageData (acc, (void *)rawdata, acc->widthStep);


        final=(unsigned char *) malloc((2*radio+1)*(2*radio+1));
        finalscaled=(unsigned char *) malloc(30*30);

        finalimg = cvCreateImage(cvSize(radio*2+1,radio*2+1),IPL_DEPTH_8U,1);
        finalscaledimg = cvCreateImage(cvSize(height,width),IPL_DEPTH_8U,1);

        cvGetSubArr (img, finalimg, cvRect ((x-radio>0? x-radio:0),((y-radio)>0? y-
radio:0), radio*2+1, radio*2+1));

        mask=cvCreateImage(cvGetSize(finalimg),IPL_DEPTH_8U,1);
        cvSetZero(mask);
        cvCircle(mask,cvPoint(radio,radio),radio,cvScalar(255,255,255,0),-1,8,0);


        cvAnd( finalimg, mask, finalimg, 0 );

        scal=(2*radio+1)/30;

        map_matrix=cvMat( 3, 3, CV_64F, m );
        sp[0] = cvPoint2D32f(0,0);
        sp[1] = cvPoint2D32f(0,radio*2);
        sp[2] = cvPoint2D32f(radio*2,radio*2);
        sp[3] = cvPoint2D32f(radio*2,0);
        dp[0] = cvPoint2D32f(0,0);
        dp[1] = cvPoint2D32f(0,width-1);
        dp[2] = cvPoint2D32f(height-1,width-1);
        dp[3] = cvPoint2D32f(height-1,0);

        cvWarpPerspectiveQMatrix( sp, dp, &map_matrix );
        m[8] = 1.; // workaround for the bug


        cvWarpPerspective( finalimg,finalscaledimg, &map_matrix,
CV_INTER_LINEAR+CV_WARP_FILL_OUTLIERS,cvScalarAll(0));


        cvEqualizeHist(finalscaledimg,finalscaledimg);


  cvNamedWindow( "image", 1 );
  cvNamedWindow( "images", 1 );
  cvNamedWindow( "imagesx", 1 );
  cvNamedWindow( "imagesy", 1 );
  cvNamedWindow( "imagesxy", 1 );
  cvShowImage( "images", modulo );
  cvShowImage( "image", finalimg );
  cvShowImage( "imagesx", imgsx);
  cvShowImage( "imagesy", imgsy);
  cvShowImage( "imagesxy", finalscaledimg);
  cvWaitKey(0);

  cvDestroyWindow("image");
  cvDestroyWindow("images");
  cvDestroyWindow("imagesx");
  cvDestroyWindow("imagesy");
  cvDestroyWindow("imagesxy");
        free(rawdata);
        cvReleaseImage(&imgsx16);
        cvReleaseImage(&imgsy16);
        cvReleaseImage(&imgs);

        free(modulos);
        free(modul);
        free(a);
        free(final);
        return(finalscaledimg);

}


IplImage* interfaz( IplImage* img, CvSeq* circular, CvSeq* triangular )

{
        IplImage* imagen;
        IplImage* panel;
        IplImage* modelo;
        IplImage* salida;
        int j,num;
        structClass *st;

        imagen = drawSquares(img,circular);
        imagen = drawSquares(imagen,triangular);

        panel = cvLoadImage("panel.jpg",3);

        salida = cvCreateImage(cvSize( imagen->width + 300, imagen->height ), 8, 3);

        cvSetImageROI(salida,cvRect(150,0,imagen->width,imagen->height));
        cvResize(imagen,salida,CV_INTER_LINEAR);
        cvResetImageROI(salida);

        cvSetImageROI(salida, cvRect(0,0,150,panel->height));
		cvResize(panel, salida,CV_INTER_LINEAR);
		cvResetImageROI(salida);

		cvSetImageROI(salida, cvRect(imagen->width + 150,0,150,panel->height));
		cvResize(panel, salida,CV_INTER_LINEAR);
		cvResetImageROI(salida);

		for (j=0; j<circular->total; j++)
		{
			st =(structClass*)cvGetSeqElem(circular , j);
			num = st->clase_final;

			if(num == 3){
				modelo = cvLoadImage("f_pelota.jpg",3);
				cvSetImageROI(salida, cvRect(imagen->width +
180,10,90,100));
				cvResize(modelo, salida,CV_INTER_LINEAR);
				cvResetImageROI(salida);
			}
			if(num == 4){
				modelo = cvLoadImage("f_hueso.jpg",3);
				cvSetImageROI(salida, cvRect(imagen->width +
180,110,90,100));
				cvResize(modelo, salida,CV_INTER_LINEAR);
				cvResetImageROI(salida);
			}
			if(num == 5){
				modelo = cvLoadImage("f_smile.jpg",3);
				cvSetImageROI(salida, cvRect(imagen->width +
180,210,90,100));
				cvResize(modelo, salida,CV_INTER_LINEAR);
				cvResetImageROI(salida);
			}
		}


		for (j=0; j<triangular->total; j++)
		{
			st =(structClass*)cvGetSeqElem(triangular , j);
			num = st->clase_final;

			if(num == 0){
				modelo = cvLoadImage("f_fuego.jpg",3);
				cvSetImageROI(salida, cvRect(30,10,90,100));
				cvResize(modelo, salida,CV_INTER_LINEAR);
				cvResetImageROI(salida);
			}
			if(num == 1){
				modelo = cvLoadImage("f_gato.jpg",3);
				cvSetImageROI(salida, cvRect(30,110,90,100));
```

```
                        cvResize(modelo, salida,CV_INTER_LINEAR);
                        cvResetImageROI(salida);
                }
                if(num == 2){
                        modelo = cvLoadImage("f_tunel.jpg",3);
                        cvSetImageROI(salida, cvRect(30,210,90,100));
                        cvResize(modelo, salida,CV_INTER_LINEAR);
                        cvResetImageROI(salida);
                }

        }

        return(salida);
}
```

CD organization

The root of the CD contain the following folders:
•Source Project VC.Net 2003
•Detecta
•Memory

The "Source Project VC.NET 2003" folder contains the source code of the Aibo object detection system and real traffic sign recognition system. There is also the Microsoft Visual C .NET 2003 solution. OpenCV and MS Visual C.Net 2003 are needed in order to build the source code.

The "Detecta" folder contains the real traffic sign recognition system build and some test images. In order to test the application, one need to drag and drop any of the test images to the detecta.exe. The resulting plotting images for an example are shown in fig. 6.

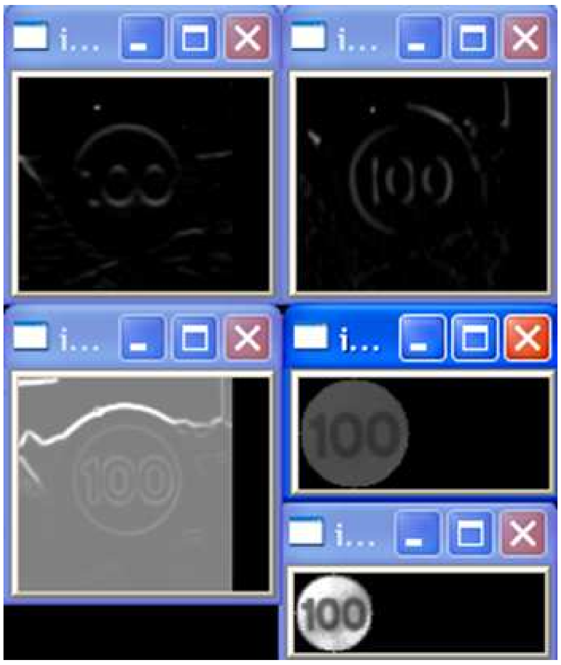

Fig. 6. Results of the executable system.

From left to right, from top to bottom:
•Y derivative
•X derivative
•Gradient of the image
•Model fitting
•Normalized model

The images remain plotted until any key is pressed. After to press any key, the system writes in the console the class membership of the input sample. If the K-NN classifies the image as 100 (speed sign), the same image normalized by the FLDA classification system is shown. Once a key is pressed, the console shows the sign label.

The "Memory" folder contains the article and documentation of the project.

Universitat
Autònoma
de Barcelona

etse

2006